

PREPRINT

Author-formatted, not peer-reviewed document posted on 19/02/2026

DOI: <https://doi.org/10.3897/arphapreprints.e189105>

New early Oligocene water frog (Anura: Ranidae: *Pelophylax*) occurrence from southeastern France

 Jasper Ponstein,  Hugues-Alexandre Blain, Hans Steur,  Jonathan Wallaard

New early Oligocene water frog (Anura: Ranidae: *Pelophylax*) occurrence from southeastern France

Jasper Ponstein^{1, 2, *}, Hugues-Alexandre Blain^{3, 4}, Hans Steur⁵, Jonathan J.W. Wallaard^{1, 6}

¹ Het Nationaal Oertijdmuseum, Bosscheweg 80, 5283 WB Boxtel, Netherlands

² Museum für Naturkunde Berlin, Invalidenstraße 43, 10115 Berlin, Germany

³ Institut Català de Paleoecologia Humana i Evolució Social (IPHES-CERCA), Zona Educacional 4, Campus Sescelades URV (Edifici W3), 43007 Tarragona, Spain

⁴ Departament d'Història i Història de l'Art, Universitat Rovira i Virgili, Avinguda de Catalunya 35, 43002 Tarragona, Spain

⁵ Laan van Avegoor 15, 6955 BD Ellecom, Netherlands

⁶ Department of Earth Sciences, Faculty of Geosciences, Utrecht University, Heidelberglaan 8, 3584 CS Utrecht, the Netherlands

* corresponding author – ponstein.jasper@gmail.com

ORCID iD: 0000-0003-0626-2565

Abstract

The widespread frog family Ranidae first appears in the European fossil record during the early Oligocene. Here we describe MAB19654, a near-complete and articulated male ranid frog skeleton from the early Oligocene Marnes du Bois d'Asson of southeastern France. The assignment of Ranidae is based on the presence of elongate posterior apophyses, cylindrical sacral apophyses and non-imbricated vertebrae. The assignment of *Pelophylax* is based on the robust humerus bearing a low crista medialis that does not reach midshaft. Additionally, we take measurements of limb bone ratios and sacral angulation of various extant osteological and fossil *Pelophylax* specimens for comparisons, and document morphological variation in the apophysis of V4. Our sample includes 58 *P. ridibundus*, 59 *P. lessonae*, 89 *P. perezi*, and one fossil *P. aquensis*, supplemented with the literature. We find that MAB19654 most closely resembles *P. ridibundus* in terms of limb bone proportions and sacral

angulation. The tarsus reduces relative to the femur in *P. perezii*, while *P. lessonae* evolves a more elongate femur and narrower sacral angulation with respect to MAB19654.

Interestingly, we find simple parallel V4 apophyses in *ridibundus+lessonae*, while complex shapes, as in MAB19654, are prevalent in the early-branching *P. perezii*. This suggests V4 morphology was complex in early *Pelophylax* and tentatively proves useful for species determination.

Introduction

True frogs (Ranidae) dispersed into Europe from Asia following the Eocene-Oligocene faunal transition or “Grande Coupure” (Yuan et al. 2016; Chan and Brown 2017; Dufresnes et al. 2024), at around 33.4 Ma (Costa et al. 2011). This major extinction event, caused by climate cooling (e.g., Ivany et al. 2000), resulted in a reduction of anuran diversity in Europe by approximately one third (Lemierre and Orliac 2025). The Grande Coupure notably led to the extinction of the speciose Eocene genus *Thaumastosaurus* (e.g., Rage 2012; Vasilyan 2018), as well as extirpations within Palaeobatrachidae in Western Europe (Venczel et al. 2013).

Subsequently, the ranid genus *Pelophylax* – Palearctic water frogs – spread out over Europe by the earliest Oligocene (MP21-22, Lemierre et al. 2022; Dufresnes et al. 2024). Published Oligocene material of *Pelophylax* is rather scarce (Fig. 1A), and consists of: 1) a partially articulated postcranial skeleton from the Upper Saproels Formation of Chartres-de-Bretagne, France (Lemierre et al. 2022); 2) fragmentary material from the Alès Basin, France (Vianey-Liaud et al. 2014); 3) the Möhren 13 site near Treuchtlingen, Germany (Sanchíz et al. 1993); and 4) the Transylvanian Basin in Romania (Venczel et al. 2024). Additionally, “*Rana aquensis*” has been reassigned to *Pelophylax aquensis* (Sanchíz 1998; Lemierre et al. 2022), which is known from the upper Oligocene of Aix-en-Provence, France (Coquand 1845; Piveteau 1927; Gaudant et al. 2018). Given the fragmentary nature of Oligocene *Pelophylax* remains, little is known about the osteology of early *Pelophylax*.

Based on molecular data, the genus *Pelophylax* underwent multiple speciation events since the early Miocene (Dufresnes et al. 2024), and now includes 14 valid extant species (Frost 2025). Additionally, numerous klepta, i.e. hybridogenetic complexes that are the result of

two different parent species producing fertile offspring, occur within *Pelophylax* (e.g., Berger 1973; Uzzell et al. 1976; Holsbeek and Jooris 2010; Dufresnes and Mazepa 2020; Dufresnes et al. 2024). Such hybrids develop an intermediate morphology, both internally and externally, between the two respective parent species (e.g., Gubányi and Korsós 1992; Mayer et al. 2013; Blain et al 2015), muddying efforts to reconstruct the ancestral character states of *Pelophylax*.

Here, we describe an articulated specimen MAB19654 of *Pelophylax*, including cranial material, recovered from the early Oligocene Marnes du Bois d'Asson of the Apt-Manosque-Forcalquier Basin, southeastern France (Fig. 1B-C). One of us (HS) collected MAB19654 in the early 1980s and kept it in his private collection, until he donated it to Nationaal Oertijdmuseum in 2024. The antiquity and completeness of MAB19654 make it an ideal specimen for assessing limb proportions and study the morphological evolution of early European water frogs in their ecological context.

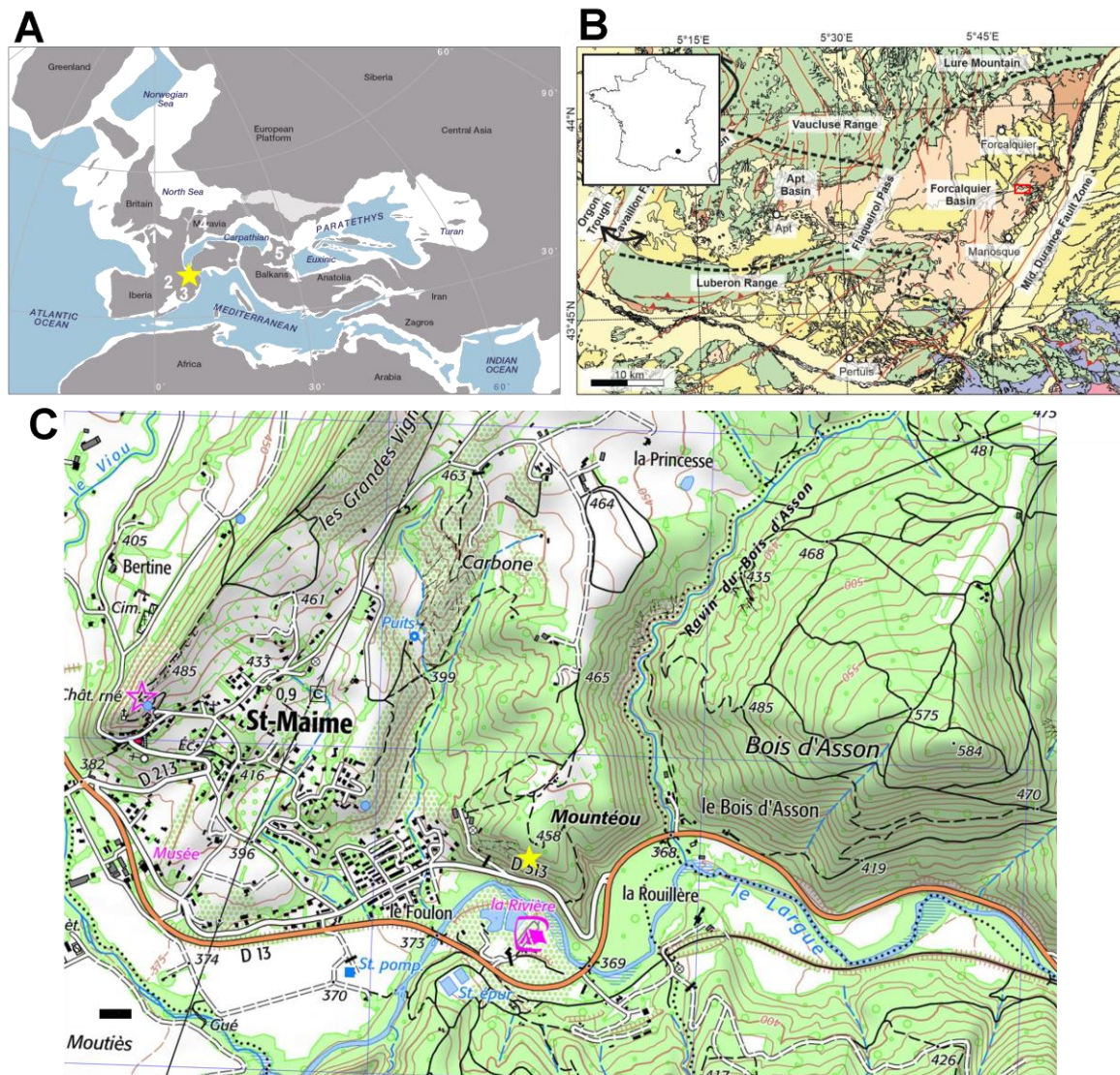


Figure 1. A palaeogeographic map of Europe during the Rupelian, showing published accounts of Oligocene specimens of *Pelophylax*. Map adopted from Palcu and Krijgsman (2023), used with permission from W. Krijgsman. 1) IGR 144547, Lemierre et al. (2022); 2) material reassigned to *Pelophylax aquensis*, Lemierre et al. (2022); 3) fragmentary material, Vianey-Liaud et al. (2014); 4) fragmentary material, Sanchíz et al. (1993); 5) fragmentary material, Venczel et al. (2024). The star denotes the location of MAB19654. B Map of the Manosque basin, adopted from Licht et al. (2024). C Topographic map of St.-Maime and Bois d'Asson. The star denotes the location of MAB19654. Map from Institut national de l'information géographique et forestière, section 3342 Manosque. Scale bar equals 100 m.

Geological setting

Geopark Luberon, which includes Bois d'Asson, has had a long history of fossil collecting dating back to the late 19th century (e.g., Oustalet 1874; Sauvage 1880; De Saporta 1891), and is known for a variety of exquisitely preserved delicate fossils such as pinecones, butterflies and feathered songbirds (e.g., Coster and Legal 2021). The Marnes du Bois d'Asson is an approximately 350 m thick sequence of sandy marls and sandstone, and occasional conglomerates (Destombes 1962). Bundles of fatty lignite are present throughout, in proximity to the site (Destombes 1962). Ducreux et al. (1985) dated the age of Marnes de Bois d'Asson to the Antoingt biozone of the latest Rupelian (early Oligocene), coeval to Marnes du Viens, based on the presence of teeth of the theriomorph rodent genera *Archaeomys* and *Issiodoromys*. MAB19654 was found in an otherwise fossil-poor, at least 10 cm thick layer of sandy marl.

Sediments of the Apt-Manosque-Forcalquier basin are deposited in a large subtropical lake environment (Schuler and Sittler 1976; Gaudant 1978; Ducreux et al. 1985). The presence of fossil shells from the marine gastropod *Potamides* suggests brackish influences (Gaudant 1978). Collection on-site (pers. obs. HS) yielded numerous cyprinodontiform fish (genus *Dapalis*) and yet undetermined insect fossils. Diverse macroflora fossils are well-known around Bois d'Asson (De Saporta 1891) but have not been documented near the outcrop (pers. obs. HS).

Materials and Methods

Specimen

We follow the English anatomical terminology of Ecker (1864, translated into English 1889) of his description of *Pelophylax* kl. *esculentus* (therein *Rana esculenta*). The fossil frog is now housed at the Nationaal Oertijdmuseum in Boxtel, Netherlands, under the reference number MAB19654. It is composed of a slab and counter-slab heralding a nearly complete and articulated frog skeleton, with a snout-vent length of 64.8 mm (Fig. 2). The main slab preserves the appendicular bones and the skull, parts of the pelvic girdle along with the imprint of the vertebral column. We label this Slab A, and denotes the field-up position. The counter-slab, hereafter Slab B preserves the vertebral column, parts of the pelvic girdle and

imprints of the appendicular bones and the skull. The slab is composed of two parts that were later joined together. The piece containing the postcrania was found first *ex situ*. A few hours later, the second piece comprising the skull was discovered *in situ* inside the steep wall (pers. obs. HS). The presence of a crista medialis on the humerus on Slab B (Fig. 2) indicates the specimen is male (e.g., Ecker 1864). Moreover, we identify this humerus as the left humerus, based on the position of the ventrally oriented humeral condyle and the crista medialis. Consequently, our terminology of left and right reflects the frog's natural position.

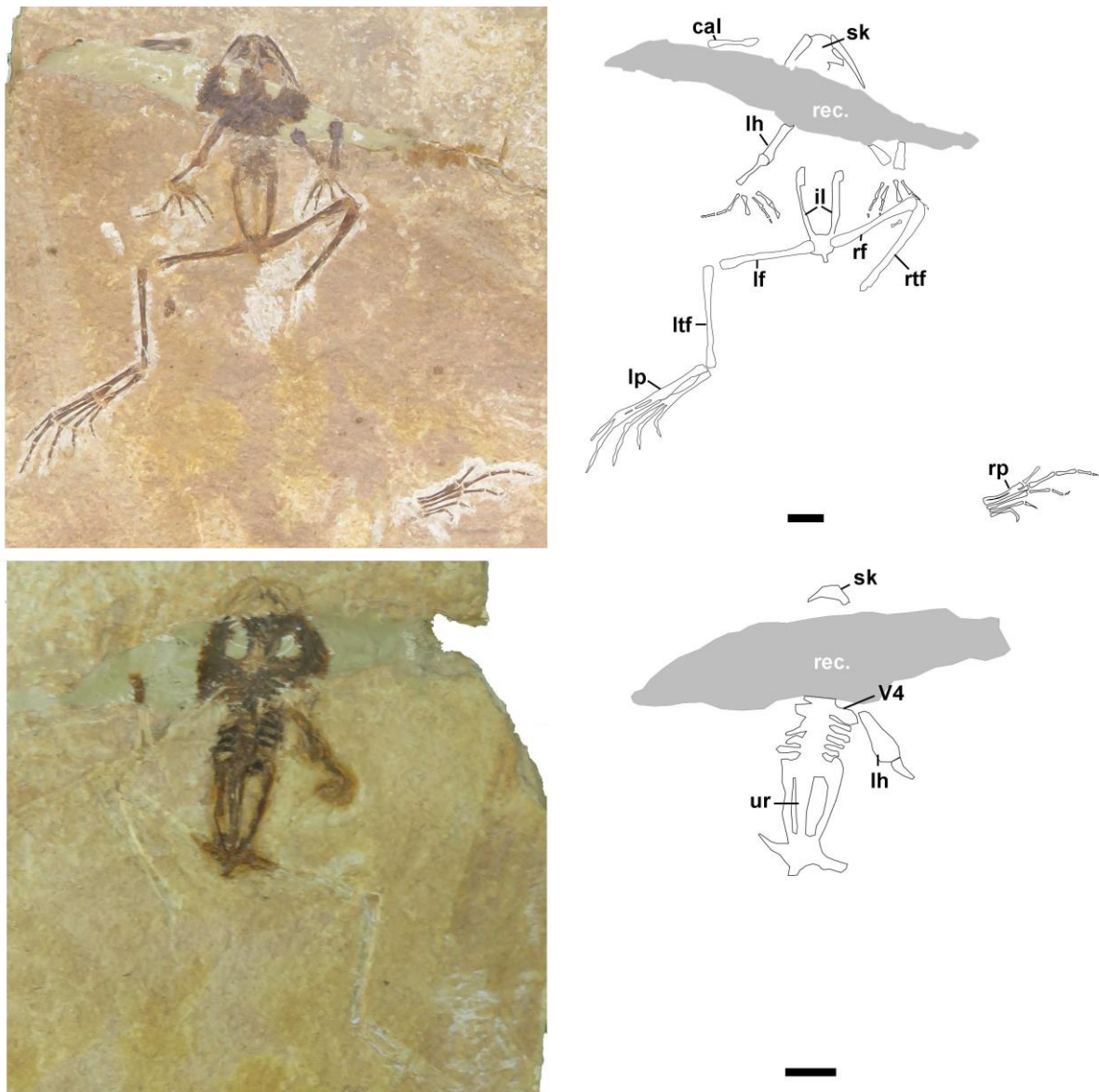


Figure 2. Overview of MAB19654 from the early Oligocene of the Manosque basin. Top: Slab A, photograph and interpretative drawing. Bottom: Slab B, photograph and interpretative drawing. Abbreviations: rec. reconstructed; cal. calcaneum; il. ilium; lf. left femur; lh. left

humerus, lp. left pes; ltf. left tibiofibula; rf. right femur, rp. right pes, rtf. right tibiofibula, sk. skull; ur. urostyle; V4. dorsal vertebra 4. Scale bar equals 1 cm.

Most of the skeleton is complete, with limited disarticulation. The anterior half of skull is preserved on Slab A. Both forelimbs are preserved from approximately the midshaft of humerus and further distally. Bones of the left forelimb are exposed on both Slab A and Slab B, whereas the right forelimb is preserved only on Slab A. While the left forelimb is articulated, in the right forelimb the humerus and radioulna are dislocated slightly. The vertebral column is present from V4 to the sacral vertebra (sacrum; V9), and better preserved on Slab B. From V4, only the left apophysis is visible. The bones of the pelvic girdle are well-preserved on Slab B. Both hindlimbs are in articulation with the pelvis, and fully exposed on Slab A. In the right limb, the knee joint is still in articulation. However, the right pes, with articulated metatarsals and phalanges has been distanced. The right calcaneum is located to the left of the skull. On the other hand, the left tibiofibula is slightly distanced from the left femur but fully articulates with the left pes. This mode of preservation reflects a “stick ‘n peel” taphonomy (Orr et al. 2016). In this particular case, the frog carcass would have been adhered to the substrate from head to torso, and the distal limb elements displaced by water currents.

The posterior part of the skull, as well as the pectoral girdle and V1-V3 have not been recovered.

Institutional abbreviations:

MAB Het Nationaal Oertijdmuseum, Boxtel, Netherlands; **MfN** Museum für Naturkunde Berlin, Berlin, Germany; **MNCN** Museo Nacional de Ciencias Naturales, Madrid, Spain; **MNHN** Muséum national d’Histoire naturelle, Paris, France; **IGR** Institut de Géologie de Rennes, Rennes, France.

Measurements

We perform a series of measurements (Table 1) on MAB19654. Sacral angulation has been used to discriminate between the two common European ranid genera *Pelophylax* and *Rana*

(Böhme 2001), and limb bone ratios have been used to distinguish between extant *Pelophylax* species within a population (e.g., Gubányi and Korsós 1992; Crochet et al. 1995; Mayer et al. 2013). Both variables have broader biomechanical ramifications as well. A wider sacral angle is correlated with improved walking and hopping capabilities, while jumpers are characterised by a narrower sacral angle (Jorgenson and Reilly 2013; Leavey et al. 2023). Moreover, hind limb osteology is indicative of both locomotion type (Jorgenson and Reilly 2013; Enriquez-Urzelai et al. 2015; Lires et al. 2016; Gómez and Lires 2019; Moen 2019; Buttner et al. 2020; Petrović et al. 2021; Leavey et al. 2023; Perez-Ben et al. 2024) and microhabitat use (e.g., Citadini et al. 2018; Stepanova and Womack 2020; Ponssa et al. 2025). Despite this body of work, the link between limb bone osteology and locomotion or microhabitat use in *Pelophylax* remains underexplored in an evolutionary context.

Table 1. Measurements taken in this study.

Measurement	Abbreviation	Source
Snout-vent length / first toe length	SVL/FtL	Gubányi and Korsós 1992
Snout-vent length / femur length	SVL/FL	Gubányi and Korsós 1992
Snout-vent length / tibiofibular length	SVL/TFL	Gubányi and Korsós 1992; Mayer et al. 2013
Femur length / tibiofibular length	FL/TFL	Gubányi and Korsós 1992
Femur length / tarsal length	FL/ACL	-
Angle between sacral apophyses	SA	Böhme 2001

Published measurements on limb proportions in *Pelophylax* have been taken exclusively from live specimens (Gubányi and Korsós 1992; Mayer et al. 2013) or wet specimens (Crochet 1995). We took measurements from dry osteological specimens instead, and test whether measurements from bones and live specimens can be used interchangeably. Our sample includes 58 disarticulated osteological specimens of *P. ridibundus* (MfN), 59 disarticulated specimens of *P. lessonae* (MfN), 89 disarticulated specimens of *P. perezi* (MNCN) and 25 disarticulated specimens of *Rana* spp. (MfN). The specific designation of *P. ridibundus* and *P. lessonae* was verified genetically. The osteological collections contain both dry bone specimens and specimens with cartilage preserved. We only calculated ratios either when femur and tibiofibula were both dry, or when both femur and tibiofibula were

cartilage-capped. Snout-vent length data was available for some of the *P. perezii* specimens, but not for the other taxa. We supplemented this data with 20 specimens of the Miocene *P. pueyoi*, taken from Sanchíz y Gil de Avalle (1977), two specimens of *P. meriani*, taken from Von Meyer (1860) and one specimen of *P. aquensis* (MNHN-F-AC1876-297). For the fossil specimens MAB19654 and MNHN-F-AC1876-297, we measure ratios for both the left and right sides to minimise potential biases from taphonomic distortion and asymmetry. We could not perform iliac measurements (used in e.g., Sanchíz et al 1993; Blain et al. 2015) on MAB19654, as the ilium in this specimen is not preserved in lateral view.

Moreover, we qualitatively characterised the shape of the apophysis of V4 (Fig. 3). Blain et al. (2024) noted variation in V4 morphology between Miocene and Pliocene fossil assemblages, as well as in extant *Pelophylax*. Here we define four morphotypes: In a parallel morphology, the anterior and posterior edge of the apophysis remain parallel along its entire length. We discriminate between a parallel morphology with a narrow apophysis (1) and a broad apophysis (2). In a trapezoid morphology (3), the two edges divert proximal to the midline, resulting in a triangular outline. In a spatulate morphology (4), the edges are parallel proximally and diverge towards the distal end.

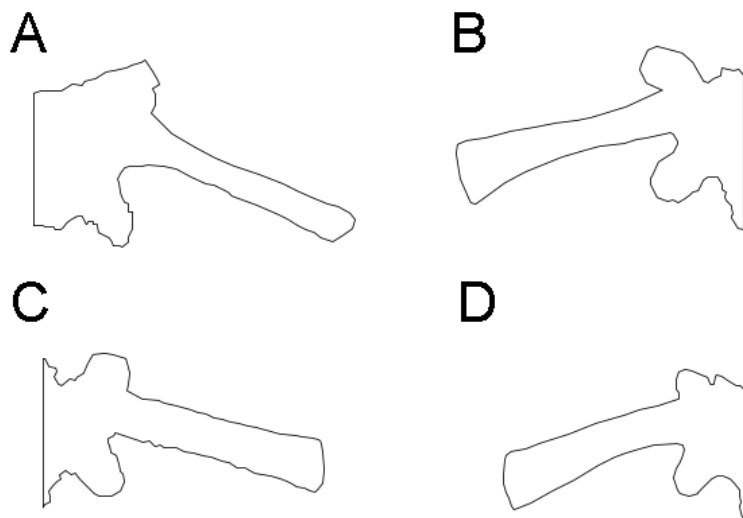


Figure 3. Line drawing of V4 morphology. A narrow parallel morphology (*Pelophylax ridibundus* MfN188), B spatulate morphology (*Pelophylax perezii* MNHN13399), C wide parallel morphology (*Pelophylax perezii* MNHN13389), D trapezoid morphology (*Pelophylax perezii* MNHN13383).

We read the raw measurements (Supplementary File 1) into the statistical computing environment R (R Core Team 2021). First, we plot the distributions of biometric measurements per species in boxplots (Tukey 1977). To test for significant interspecific differences in biometric measurements, we use a Bonferroni corrected pairwise t-test of the stats package (R Core Team 2021). Intraspecific variation and, when possible, variance between dry bones, cartilage-capped bones and live specimens were done using a Welch Two Sample t-test and a Levene-test using the car-package (Fox et al. 2019), respectively. The occurrence data of V4 apophysis morphologies are visualised in pie charts using ggplot2 (Wickham 2016). Lastly, we used the sample of *P. perezi* to determine if there is no correlation between snout-vent length and tibiofibular ratio (Pearson's $r = 0.02$; $p = 0.92$), justifying the combined use of juvenile and adult specimens.

Systematic palaeontology

LISSAMPHIBIA Haeckel, 1866

ANURA Duméril, 1805

NEOBATRACHIA Reig, 1958

RANOIDEA Rafinesque, 1814

RANIDAE Batsch, 1796

PELOPHYLAX Fitzinger, 1843

Description

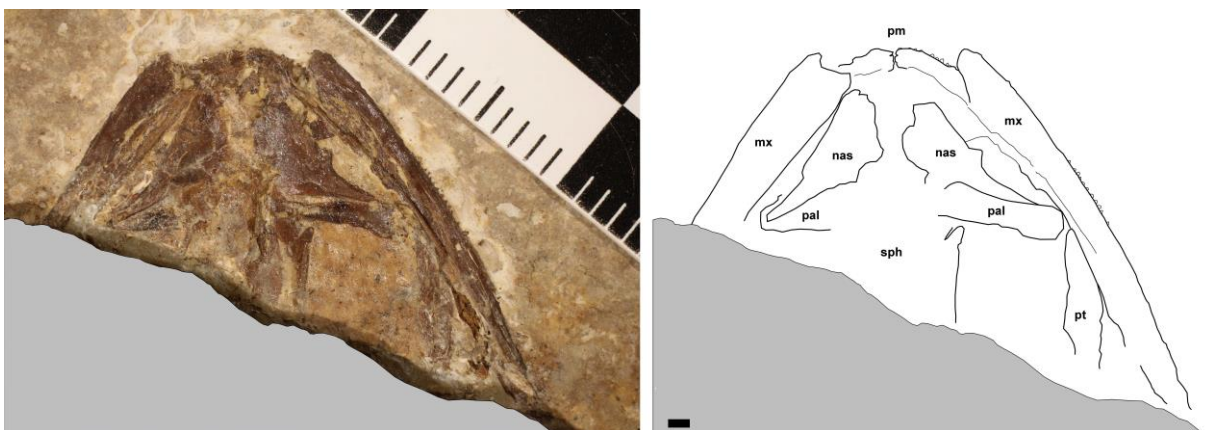


Figure 4. Skull osteology of MAB19654 from the early Oligocene of the Manosque basin on Slab A, photograph and interpretative drawing. Abbreviations: mx. maxilla; nas. nasal; pm. premaxilla; pt. pterygoid; sph. sphenethmoid. Scale bar equals 1 mm.

Cranium

The bones of the anterior half of skull are preserved in ventral view on Slab A, but largely disarticulated (Fig. 4). Both premaxillae are articulated as paired element, and the midline suture is visible. There are approximately 10 tooth positions present on the right premaxilla. The maxillae are present on both sides as elongate and stiff, smooth, rods. Dermal bones, including the maxilla, are distinctly ornamented in Pelobatidae (Roček et al. 2014) and *Thaumastosaurus* (Laloy et al. 2013; Vasilyan 2018; Lemierre et al. 2021; Georgalis et al. 2023), but this feature may not be visible in ventral view. Numerous conical teeth are preserved on the lateral side of the right maxilla of MAB19654 (Fig. 4). This condition differs from Bufonidae, which are characterised by an edentulous maxilla (Sánchez y Gil de Avalle 1977; Bailon 1999). Both nasal bones are present as roughly equilateral triangles but disarticulated and not fused at the midline. The palatines are present posterior to the nasals, as elongated struts that extend from the midline of the sphenethmoid to the maxillae. On the left side, the nasal is slightly tilted to cover the lateral portion of the palatine. Only the anterior part of the sphenethmoid is preserved, but its details are not visible. Anurans have a paired, triradial pterygoid (e.g., Bailon 1999), of which only the anterior branch is preserved in MAB19654. The anterior branch of the right pterygoid is slender, as in *P. pueyoi* (Blain et al. 2023). Moreover, the absence of an alar expansion of the pterygoid is typical for Ranidae (Bailon 1999; Blain et al. 2024).

Slab B preserves an imprint of the maxillae (Fig. 2). A splint of the dentary and angular bones is present on the right side.

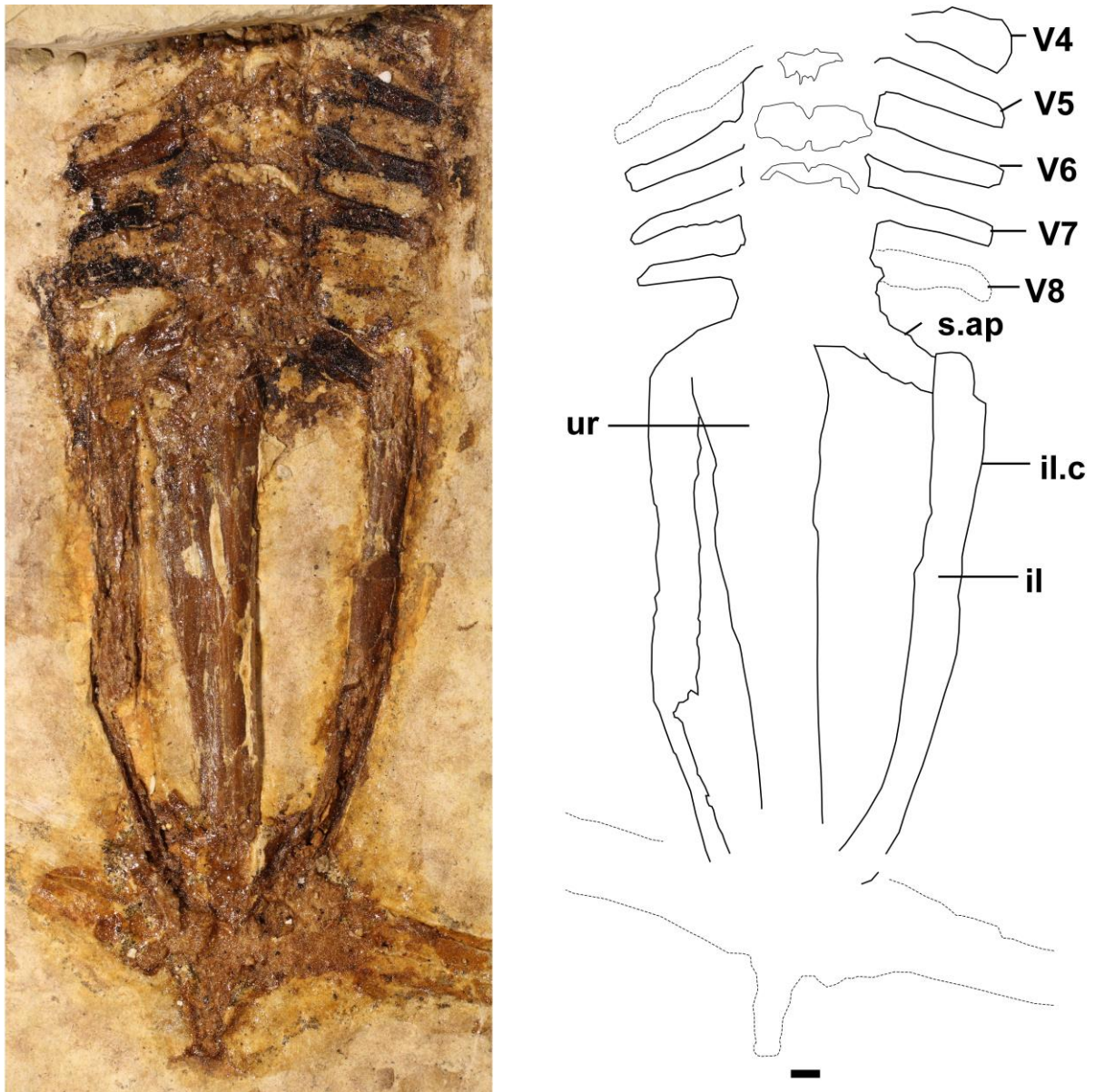


Figure 5. Vertebral column osteology of MAB19654 from the early Oligocene of the Manosque basin on Slab B, photograph and interpretative drawing. Abbreviations: il. ilium; il.c. iliac crest; s.ap. sacral apophysis; ur. urostyle; V4-V8. dorsal vertebrae 4-8. Scale bar equals 1 mm.

Vertebral column

The vertebral column is best visible on Slab B (Fig. 5). Slab A and B are split roughly at the interface between the vertebral centra and the neural spines. Six vertebrae are preserved (from V4 to sacrum) and lack free ribs. Ranidae and Bufonidae are characterised by the absence of free ribs in both subadult and adult individuals, unlike alytids that retain free ribs on V2, V3 and V4 (Sanchíz y Gil de Avalue 1977). On Slab A, the ventral portion of the neural

spines are visible and appear not imbricated like in other ranids (Sanchíz y Gil de Avalor 1977; Blain et al. 2023) and *Thaumastosaurus* (Georgalis et al. 2023). The vertebrae of Alytidae, Pelobatidae, Bufonidae and Palaeobatrachidae are imbricated (Sanchíz y Gil de Avalor 1977; Roček et al. 2021). Slab B shows the vertebral centres in dorsal view, but their delineation cannot be discerned. The left diapophysis of V4 is broad and has a trapezoid outline (Fig. 5), as it is typical in *P. pueyoi* and *P. quellebergi* (Navás 1920, 1922; Sanchíz y Gil de Avalor 1977; Blain et al. 2024). It appears to be significantly wider than in the extant *Pelophylax* *kl. esculentus* specimen described by Ecker (1864), the Oligocene IGR 144547 (Lemierre et al. 2022) and the Pliocene *Pelophylax* spp. (Blain et al. 2024). All observed specimens of *Thaumastosaurus* preserving a vertebral column display a wide parallel V4 morphology (Laloy et al. 2013; Lemierre et al. 2021). The diapophyses of V5-V8 are roughly cylindrical and relatively long, equal in length to V4. In Palaeobatrachidae, *Thaumastosaurus*, Alytidae and Pelobatidae, the posterior diapophyses are short to very short (Sanchíz y Gil de Avalor 1977; Roček et al. 2014; Lemierre et al. 2021). All visible diapophyses in MAB19654 are inclined slightly posteriorly – diapophysis 6 on the left is dislocated to be inclined slightly more. There is a single sacral vertebra (V9), which is not fused to V8. The transverse processes of the sacral vertebra are nearly twice as wide as diapophyses of V5-V8, but cylindrical with straight margins (Fig. 5). This is a diagnostic feature of Ranidae (Böhme 1977; Sanchíz y Gil de Avalor 1977; Bailon 1999; Kruzhkova and Kovalenko 2010), but also seen in *Thaumastosaurus* (Laloy et al. 2013; Lemierre et al. 2021). It differs greatly from the anteroposteriorly expanded, fan-like, transverse processes present in Bufonidae, Pelobatidae, Alytidae (Böhme 1977; Sanchíz y Gil de Avalor 1977; Bailon 1999; Kruzhkova and Kovalenko 2010) and Palaeobatrachidae (Roček et al. 2021). On the left side of B, the distalmost part of the transverse process is overlain by the ilium. The angulation between both transverse processes in MAB19654 is 125°.

The urostyle of MAB19654 is a rod-like element without transverse processes (Fig. 5). It is exposed in lateral view on Slab B, with the dorsal ridge pointing to the frog's right side. This position suggests the urostyle has been flipped over, so that its proximal end was not fused to the sacral vertebra. An unfused urostyle lacking transverse processes is characteristic of Ranidae (Sanchíz y Gil de Avalor 1977). Alytidae possess transverse processes on the urostyle, whereas the urostyle fuses to the sacrum in subclades of Pelobatidae and

Bufonidae (Sanchíz y Gil de Avalle 1977). The dorsal ridge of the urostyle runs from the anterior extremity of the urostyle to roughly two thirds of its length, and gradually reduces dorsoventral height posteriorly, similar to extant *Pelophylax* kl. *esculentus* (Ecker 1864). This ridge is tall, like in *Pelophylax* kl. *esculentus* (Bailon 1999). The morphology of the ridge is more variable interspecifically in *Rana*, as it is relatively low in *R. arvalis*, *R. pyrenaica* and *R. temporaria*, but tall in *R. dalmatina* and *R. iberica* (Bailon 1999; Blain and Arribas 2017). In Bufonidae and Pelobatidae, such a ridge is absent (Bailon 1999). Additionally, the ventral surface of the urostyle in MAB19654 appears straight (Fig. 5), as in *Pelophylax* kl. *esculentus* (Ecker 1864). In the *Rana* specimens figured by Bailon (1999), this surface is strongly curved.

Pectoral girdle

Not present.

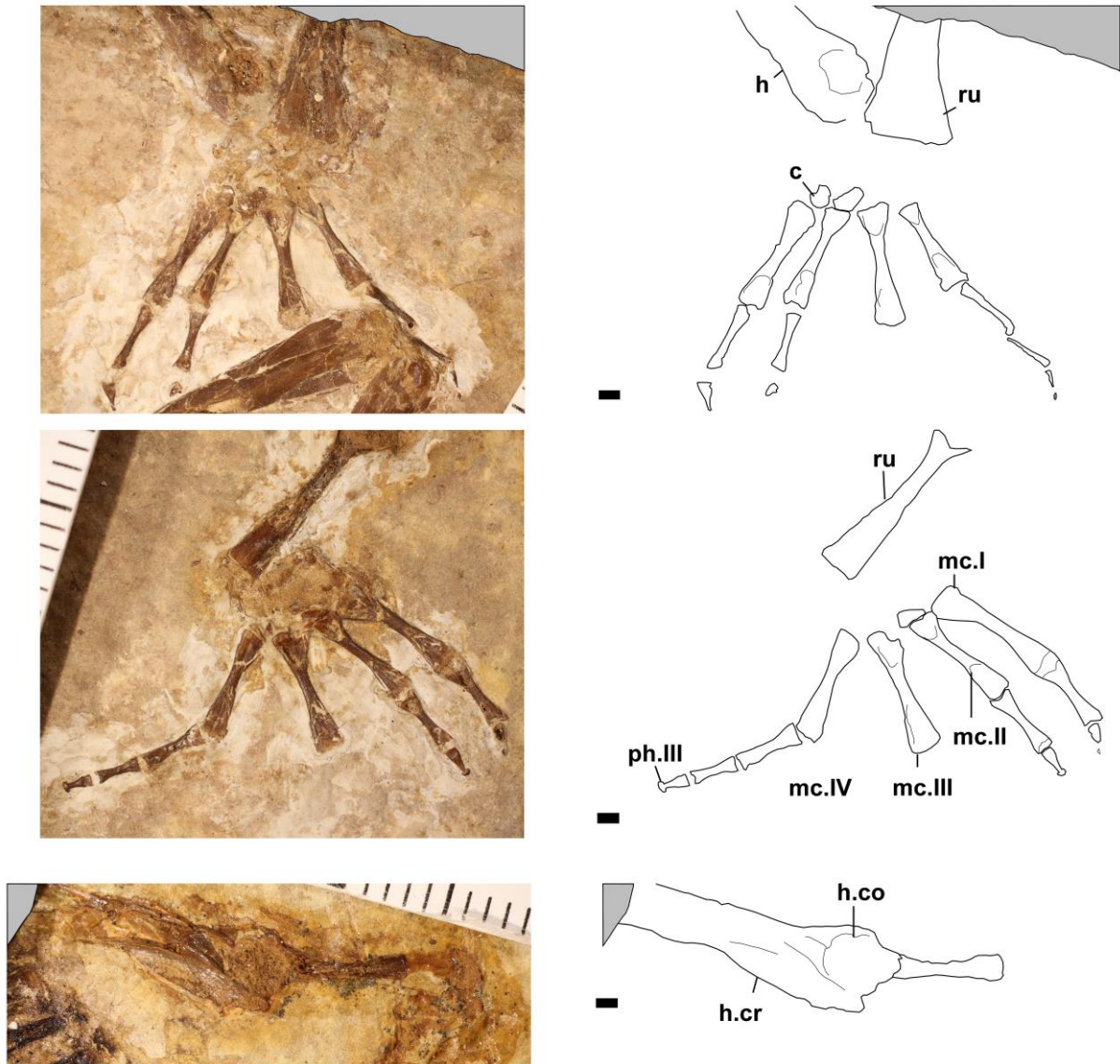


Figure 6. Manus osteology of MAB19654 from the early Oligocene of the Manosque basin. Top row right manus on Slab A, photograph and interpretative drawing, middle row left manus on Slab A, photograph and interpretative drawing, bottom row left manus on Slab B, photograph and interpretative drawing. Abbreviations: c. semilunar carpal-like bone; h. humerus; h.co. humeral condyle; h.cr. crista medialis; mc.I-mc.IV. metacarpal I-IV; ph.III. phalanx III; ru. radioulna. Scale bar equals 1 mm.

Forelimbs

The distal halves of both humeri are preserved, on both slabs (Fig. 6). As such, the articulation with the scapulae is not present. The left humerus on Slab B shows the most details (Fig. 6). A cross-section of the condyle is visible distally, indicating this humerus is preserved in ventral view. It is circular and aligns with the diaphysis, as is typical for Ranidae

(Bailon 1999). Medially to the condyle is a prominent crista medialis, providing evidence the specimen is male. This crest is straight, with its height roughly equal to the width of the humeral shaft. Similar to *Pelophylax* and unlike *Rana*, the crest in MAB19654 does not reach past the midpoint of the diaphysis (Bailon 1999). The diaphysis of the humerus is straight and rather robust (Fig. 6) like in *Thaumastosaurus* (Laloy et al. 2013) and *Pelophylax* (Bailon 1999; Ratnikov 2001). By contrast, the humeral diaphysis in Bufonidae and Alytidae is curved (Bailon 1999). In *Rana*, the shaft of the humerus is slender, less wide than the humeral condyle (Bailon 1999; Ratnikov 2001). On Slab A, the distal part of right humerus is preserved in dorsal view, exposing the condyle scar. The radius and ulna are fused into the radioulna, forming a relatively short bone. Anteriorly, the olecranon is obscured by the condyle of the humerus. Slab A shows the two tubes corresponding to the ulna and radius in lateromedial view of the right radioulna, with a distinct notch running medially. On the right side, the radioulna is preserved in dorsoventral view and appears a much narrower bone.

The bones of the manus of MAB19654 are preserved on Slab A (Fig. 6). The carpal bones appear to be missing, though a semilunar carpal bone might be present on the right manus on Slab A (Fig. 6). The four preserved metacarpals in MAB19654 are of roughly equal length and about half the length of the radioulna (Fig. 6). Palaeobatrachidae have more elongate metacarpals, measuring three-quarters or more of the radioulna length (Roček et al. 2021). The second metacarpal of *Thaumastosaurus gezei* MNHN-QU 17279 is significantly longer than the other metacarpals (Laloy et al. 2013). Four digits are present in each manus of MAB19654, corresponding to digits II-V (Fig. 6). The strongly reduced digit I, consisting only of a metacarpal (os lunatum; Ecker 1864) is not preserved. Digit II and III consist of the metacarpal and two phalanges. The fourth digit is not well preserved on either manus. Digit V is the longest with three phalanges preserved on the left side, resulting in a phalangeal formula of 2-2-3-? (Fig. 6). The distalmost phalanges bear a knob distally (Fig. 6), similar to IGR 144547 (Lemierre et al. 2022). A stray phalanx, not a distal phalanx, is located within the right femur-tibiofibula articulation on Slab A, but it is unclear which digit it derives from.

Pelvic girdle

Both ilia are preserved (Fig. 5). They have been split transversally, and the bone is exposed on both Slab A and Slab B. The ilia form a roughly V-shaped outline. An incipient dorsal crest

is visible on the right ilium anteriorly on Slab A and its imprint on Slab B (Fig. 5 Vertebral column). The dorsal crest is tall in *Pelophylax* (Von Meyer 1860; Bailon 1999; Blain et al. 2024) and *Thaumastosaurus* (Georgalis et al. 2023), varies interspecifically within *Rana* (Bailon 1999; Blain and Arribas 2017) but is low in Palaeobatrachidae (Roček et al. 2021) and lacking in Pelobatidae (Roček et al. 2014). However, due to the positioning of the ilium of MAB19654 in the sediment, the full extent of the crest could not be assessed. Anteriorly, the ilia overlie sacral apophyses on Slab B. The ilia contact each other posteriorly at the ischiopubis on both slabs. A short pubic process projects posteriorly.

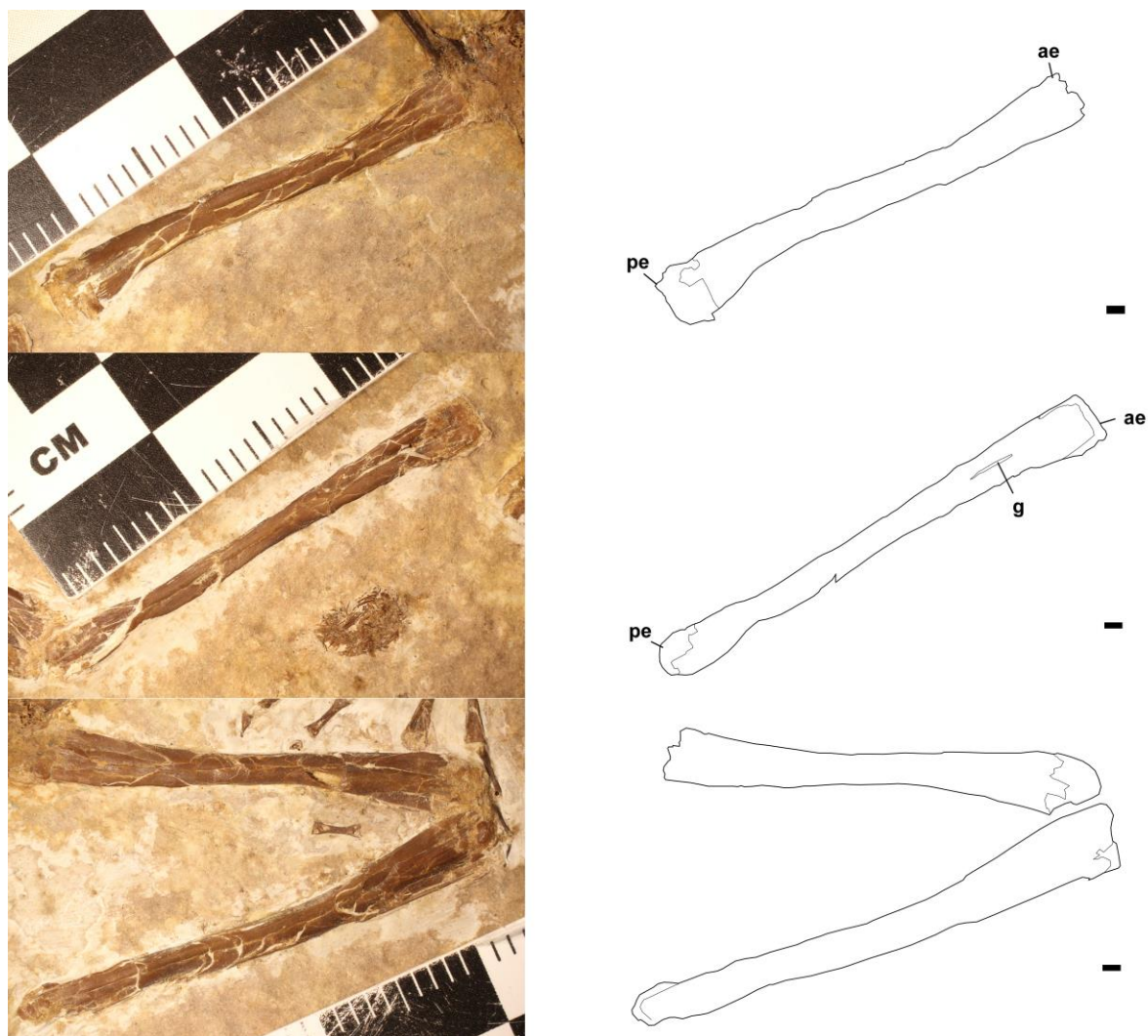


Figure 7. Hindlimb osteology of MAB19654 from the early Oligocene of the Manosque basin. Top row left femur on Slab A, photograph and interpretative drawing, middle row left tibiofibula on Slab A, photograph and interpretative drawing, bottom row right hindlimb, photograph and interpretative drawing. Abbreviations: ae. anterior extremity; g. groove; pe. posterior extremity. Scale bar equals 1 mm.

Hindlimbs

The bones of the hindlimbs are preserved three-dimensionally on Slab A (Fig. 7), while Slab B clearly shows the imprint. Proximally, the femora articulate with the pelvis. Both femora are relatively short with respect to snout-vent length, compared to modern *Pelophylax* species (e.g., Gubányi and Korsós 1992; Mayer et al. 2013). The outline is slightly sigmoid (Fig. 7). Both proximal and distal ends are slightly wider than the shaft. The epiphyseal surfaces appear to run parallel, unlike the femur of *Pelobates cultripes* in which the proximal epiphyseal surface makes a clear angle with respect to the distal surface (Bailon 1999). There is no crest present on the femoral shaft, nor medial or lateral margins (Fig. 7), unlike in alytids and bufonids (Bailon 1999). Moreover, the femur of MAB19654 is gracile unlike the robust femur of Bufonidae (Bailon 1999). The length ratio between the femur and tibiofibula amounts 0.894 for the left side and 0.933 for the right side; the tibiofibula is the longer bone. Both tibiofibulae are preserved as straight elongate rods. In both Bufonidae and Pelobatidae, by contrast, the proximal and distal ends of the tibiofibula are visibly wider than the shaft (Bailon 1999), resulting in an hourglass-outline. Moreover, the bufonid tibiofibula is more robust than that of Ranidae (Bailon 1999; Ratnikov 2001). The left tibiofibula of MAB19654 bears a shallow groove proximally (Fig. 7), denoting the separation between the fused tibia and fibula as seen in anteroposterior view (Bailon 1999).

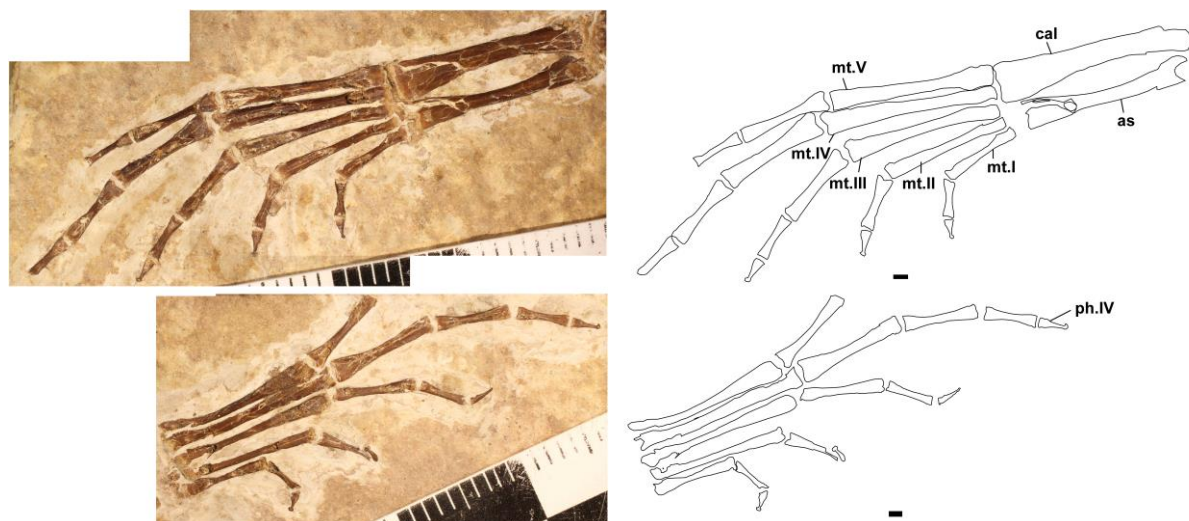


Figure 8. Pes osteology of MAB19654 from the early Oligocene of the Manosque basin. Top row left pes on Slab A, photograph and interpretative drawing, bottom row right pes on Slab A, photograph and interpretative drawing. Scale bar equals 1 mm.

Both tarsal elements are preserved on the left hindlimb (Fig. 8). At midshaft, the astragalus and calcaneum divert, but they approach each other proximally and distally. The shaft of the calcaneum is wider than that of the astragalus (cf. Ecker 1864). Distally, the astragalus and calcaneum articulates with metatarsals on left limb (Fig. 8). Both tarsal bones remain free along their entire length as is typical in Ranidae, but unlike the condition in Alytidae whereby the elements are fused distally (Sanchíz y Gil de Avalle 1977) or in *Pelobates cultripes*, whereby both ends fuse (Bailon 1999). The right calcaneum is distanced from the tibiofibula, preserved left to the skull on Slab A (Fig. 2). The pes bears five digits, of which Digit IV is the longest with four phalanges (Fig. 8). Digit I and II consist of two phalanges, while digit III consists of three. The total count of digit V is unclear, as the distal phalanx on neither pes is preserved. This leaves a phalangeal formula of 2-2-3-4-? (Fig. 8). Similar to what we reported in the manus, the distal end of the distal phalanges is knob-like (Fig. 8). This phalangeal shape contrasts with the description of Ecker (1864), stating that the terminal phalanges are somewhat hooked towards the plantar surface.

The astragalus and calcaneum form common epiphysis of calcified cartilage in *P. esculentus* (e.g., Ecker 1864). This is not preserved in MAB19654.

Measurements

Table 2. Overview of measurements taken in this study and published data. Abbreviations: SVL. snout-vent length; FtL. first toe length; FL. femur length; TFL. tibiofibula length; ACL. tarsal length; SA. sacral angulation. Black data cells denote missing data.

Taxon	Sex	preservation	SVL/FtL	n	SVL/FL	n	SVL/TFL	n	FL/TFL	n	FL/ACL	n	SA	n	Source
MAB19654	♂	fossil	6.36	1	2.312 - 2.314	1	2.07 - 2.16	1	0.893 - 0.933	1	1.78	1	125°	1	this study
<i>Pelophylax lessonae</i>	♀	live	8.14±0.71	66	2.13±0.09	66	2.25±0.11	66	1.06±0.05	66					Gubányi and Korsós (1992)
<i>Pelophylax lessonae</i>	♂	live	8.13±0.59	61	2.09±0.09	61	2.22±0.10	61	1.06±0.04	61					Gubányi and Korsós (1992)
<i>Pelophylax lessonae</i>	not defined	live					1.9 - 2.3	?							Mayer et al. (2013)
<i>Pelophylax lessonae</i>	not defined	dry bone					2.1±0.02								
<i>Pelophylax lessonae</i>	not defined	dry bone							0.96 - 1.009	7	1.68 - 1.93	53	94 - 125°	58	this study
<i>Pelophylax lessonae</i>	not defined	w/cartilage							0.994±0.017		1.834±0.05		110.67±7.65		
<i>Pelophylax lessonae</i>	not defined	w/cartilage							0.923 - 1.033	51					this study
<i>Pelophylax lessonae</i>	not defined	w/cartilage							0.993±0.018						
<i>Pelophylax ridibundus</i>	♀	live	6.33±0.27	11	1.90±0.11	11	1.87±0.06	11	0.99±0.04	11					Gubányi and Korsós (1992)
<i>Pelophylax ridibundus</i>	♂	live	6.22±0.38	16	1.86±0.09	16	1.82±0.06	16	0.98±0.03	16					Gubányi and Korsós (1992)
<i>Pelophylax ridibundus</i>	not defined	live					1.7 - 2.1	?							Mayer et al. (2013)
<i>Pelophylax ridibundus</i>	not defined	live					1.9±0.01								
<i>Pelophylax ridibundus</i>	not defined	wet					1.767 - 1.905	5							Crochet et al. (1995)
<i>Pelophylax ridibundus</i>	not defined	dry bone							0.879 - 0.962	40	1.72 - 2.04	21	105 - 135°	55	this study
<i>Pelophylax ridibundus</i>	not defined	dry bone							0.913±0.018		1.87±0.07		119.4±66.93		
<i>Pelophylax ridibundus</i>	not defined	w/cartilage							0.905 - 0.970	21					this study
<i>Pelophylax ridibundus</i>	not defined	w/cartilage							0.934±0.020						
<i>Pelophylax esculentus</i>	♀	live	7.35±0.46	108	2.08±0.10	108	2.10±0.10	108	1.01±0.02	108					Gubányi and Korsós (1992)
<i>Pelophylax esculentus</i>	♂	live	7.15±0.53	14	2.03±0.07	14	2.06±0.09	14	1.01±0.01	14					Gubányi and Korsós (1992)
<i>Pelophylax esculentus</i>	not defined	live					1.8 - 2.2	?							Mayer et al. (2013)
<i>Pelophylax esculentus</i>	not defined	live					2.0±0.01								
<i>Pelophylax perezi</i>	not defined	wet					1.795 - 2.247	13							Crochet et al. (1995)
<i>Pelophylax perezi</i>	not defined	dry bone							0.870 - 0.968	58	2.033 - 2.140	4	105 - 146°	84	this study
<i>Pelophylax perezi</i>	not defined	dry bone							0.903±0.017		2.090±0.045		124.35±6.64		
<i>Pelophylax perezi</i>	not defined	w/cartilage							0.898	1					this study
<i>Pelophylax grafi</i>	not defined	wet					1.742 - 2.179	8							Crochet et al. (1995)
<i>Pelophylax pueyoi</i>	not defined	fossil							0.866 - 0.968	20					Sanchíz y Gil de Avallé (1977)
<i>Pelophylax pueyoi</i>	not defined	fossil							0.91±0.02						
<i>Pelophylax aquensis</i>	not defined	fossil							0.899 - 0.916	1	1.88	1			this study
<i>Pelophylax meriani</i>	not defined	fossil							0.885 - 0.931	2					Von Meyer (1860)
<i>Rana arvalis</i>	not defined	dry bone											72 - 93°	3	Böhme (2001)
<i>Rana arvalis</i>	not defined	dry bone							0.723 - 0.923	5			95 - 124°		this study
<i>Rana arvalis</i>	not defined	dry bone							0.866±0.081	5			108.4±10.60		
<i>Rana temporaria</i>	not defined	dry bone											95 - 125°	6	Böhme (2001)
<i>Rana temporaria</i>	not defined	dry bone							0.860 - 0.923	17			102 - 132°	17	this study
<i>Rana temporaria</i>	not defined	dry bone							0.892±0.020				118.6±10.0		

The limb bone ratios in MAB19654 fit within the range observed in extant *Pelophylax* osteological specimens (Table 2). The femur-tibiofibular ratio in MAB19654, 0.893 for the right side and 0.933 for the left side, plots within the range of the extant species *P. perezi* and *P. ridibundus*, as well as the fossil *P. aquensis*, *P. meriani* and *P. pueyoi* (Fig. 9). *P. lessonae* notably has a significantly higher femur-tibiofibular ratio than of all other species (Table 2; Supplementary File 2). Regarding the femur-tarsal ratio of MAB19654, only the left metric could be measured (1.78), plotting within the lowest quartile of *P. lessonae* and, exclusively when considering outliers, in range of *P. ridibundus* (Fig. 9). The femur-tarsal ratio of *P. perezi* is significantly higher than in the other *Pelophylax* species (Table 2; Supplementary File 2).

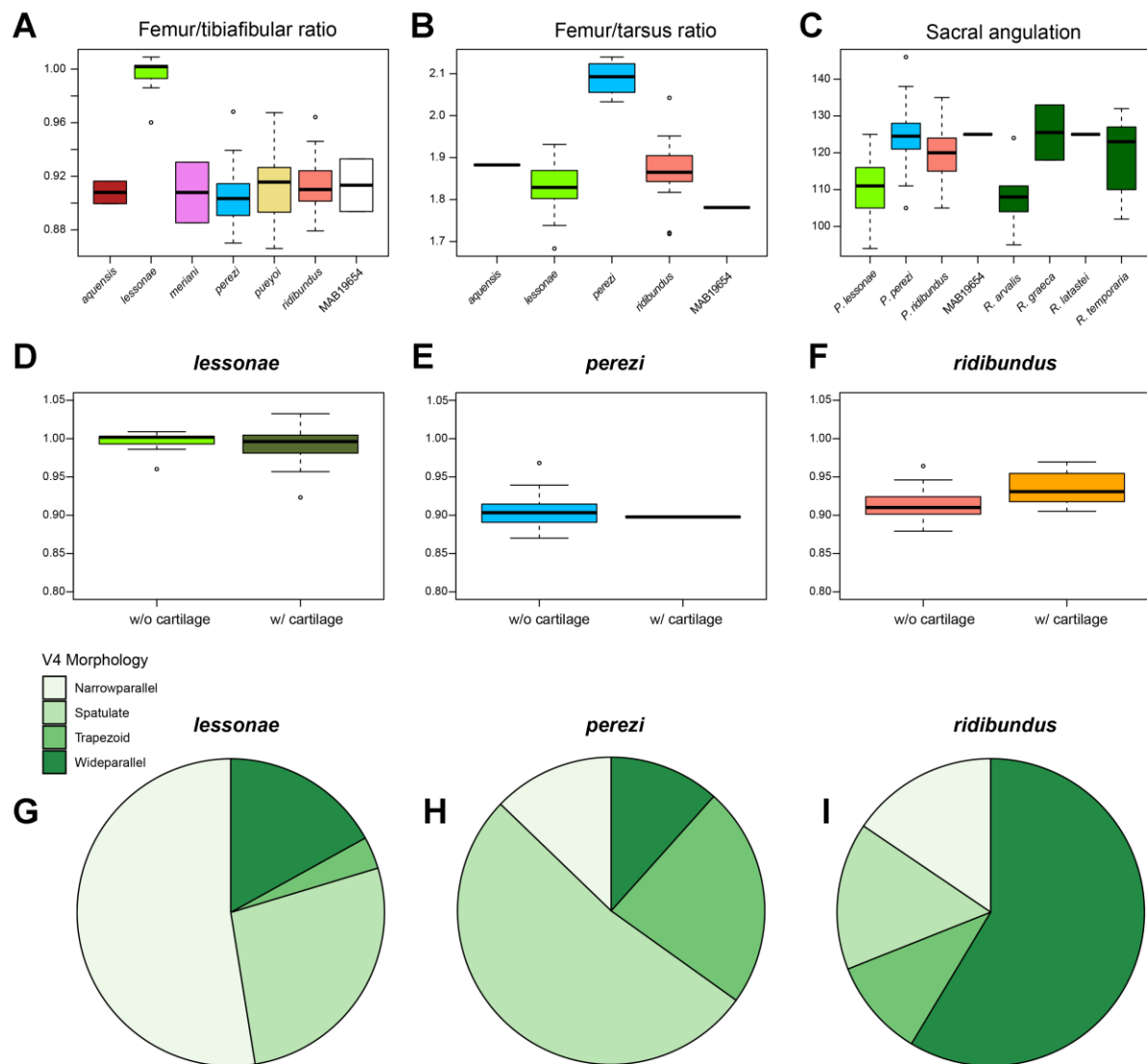


Figure 9. Overview of measurements taken in this study. A-C show boxplots of interspecific comparisons. A femur/tibiafibular ratio (dry bone only), B femur/tarsal ratio (with cartilage cap), C sacral angulation. D-F show boxplots of intraspecific comparisons of the femur/tibiafibular ratio of dry bone versus cartilage capped specimens. D *Pelophylax lessonae*, E *Pelophylax perezi*, F *Pelophylax ridibundus*. G-I show pie charts with relative distribution of V4 morphology. G *Pelophylax lessonae*, H *Pelophylax perezi*, I *Pelophylax ridibundus*

Snout-vent length to single bone element ratios are more variable between MAB19654 and the published extant *Pelophylax* populations. Snout-vent length to femur ratio in MAB19654 (2.312 – 2.314) exceeds that of the male populations in *P. lessonae* (2.09±0.09) and *P. ridibundus* (1.86±0.09) (Gubányi and Korsós 1992; Table 2). This indicates that the femur is relatively shorter in MAB19654 than in modern *Pelophylax* species. Relative tibiofibular

length of MAB19654 (2.07 – 2.16) lies within two or three standard deviations of the Bavarian population (2.1±0.2; Mayer et al. 2013) and the Hungarian male population of *P. lessonae* (2.22±0.10; Gubányi and Korsós 1992). Compared to *P. ridibundus*, the snout-vent length to tibiofibular ratio in MAB19654 greatly exceeds that of the male Hungarian population (1.82±0.06; Gubányi and Korsós 1992), the Bavarian population (1.9±0.01; Mayer et al. 2013) and diverse wet collections (1.767-1.905; Crochet et al. 1995). It does fall within the range measured in the wet collection of *P. perezi* (1.795-2.247; Crochet et al. 1995). Lastly, snout-vent length to first toe length of MAB19654 exclusively matches with that of *P. ridibundus* (6.22±0.38; Gubányi and Korsós 1992).

The sacral angulation of MAB19654 (125°) falls in the higher range of *P. ridibundus* and *P. perezi* but exceeds all measured specimens of *P. lessonae* (Fig. 9). When comparing to extant *Rana*, the sacral angulation in MAB19654 exceeds that of *Rana arvalis* but falls within the range of *R. graeca* and *R. temporaria*. With a larger sample size than Böhme (2001), we found no significant difference in sacral angulation between the genera *Rana* and *Pelophylax* ($p = 0.42$).

When comparing our dry osteological ratios with the data presented by Gubányi and Korsós (1992) on live Hungarian frog populations, we find that the femur-tibiofibular ratio is significantly different for both *P. lessonae* ($p \ll 0.005$) and *P. ridibundus* ($p \ll 0.005$), regardless of our sample is compared to the male or female population of Gubányi and Korsós (1992). This is also true for the cartilage-capped specimens of *P. lessonae* ($p \ll 0.005$) and *P. ridibundus* ($p_{\text{male}} \ll 0.005$; $p_{\text{female}} = 0.0008$). As Mayer et al. (2013) did not report number of specimens for each measurement, we could not run a t-test for their sample. Moreover, Crochet et al. (1995) reported TFL/SVL instead of SVL/TFL. To match their results with the measurements in this paper, we inversed the values published in Crochet et al. (1995) in Table 2. Within our own dataset, we observed a discrepancy between femur-tibiofibular ratio between dry osteological and cartilage-capped specimens of *P. ridibundus* ($p \ll 0.005$). In *P. lessonae*, there was no significant difference ($p = 0.817$). Additionally, the variance between the cartilage-bearing specimens and dried bone was insignificant both in *P. ridibundus* ($F = 0.8072$; $p = 0.37$) and in *P. lessonae* ($F = 0.5147$; $p = 0.48$).

All of the four defined V4 morphotypes are observed in the three sampled extant *Pelophylax* species (Fig. 9). The more complex trapezoid morphology, as observed in MAB19654, and spatulate morphologies are far more frequent in *P. perezii* (75%). Simple parallel morphologies occur more frequently in *P. lessonae* and *P. ridibundus*, with *P. lessonae* most frequently displaying the narrow parallel apophysis morphotype (52.4%) and *P. ridibundus* the wider apophysis morphotype (58.6%).

Discussion

Diagnosis

Three anuran clades are represented by partially complete or complete skeletons in the Paleogene of France; Ranidae (genera *Pelophylax* and *Rana*; Roček and Wuttke 2010; Gaudant et al. 2018; Lemierre et al. 2022), Pelobatoidea (genera *Eopelobates*, *Pelobates*; Roček et al. 2014) and Pyxicephalidae (genus *Thaumastosaurus*; Laloy et al. 2013; Lemierre et al. 2021; Georgalis et al. 2023). Additionally, fragmentary specimens are known from Palaeobatrachidae, Alytidae and Bufonidae (Rage and Roček 2003; Roček 2013).

MAB19654 differs from Pelobatoidea (Roček et al., 2014) by non-imbricated neural arches and the lack of postsacral vertebrae and associated webbed apophyses. Moreover, it differs from the Pelobatidae *Eopelobates* and *Pelobates* (Böhme 1977; Sanchíz y Gil de Avalle 1977; Bailon 1999) by the absence of an alary process on the pterygoid, posterior apophyses elongate, cylindrical sacral apophyses, urostyle not fused to sacrum, absence of transverse processes on the urostyle. MAB19654 differs from the pyxicephalid *Thaumastosaurus* (Laloy et al. 2013; Vasilyan 2018; Lemierre et al. 2021; Georgalis et al. 2023) by the lack of ornamentation on the maxilla, relatively short metacarpal bones of equal length and posterior apophyses elongate. Moreover, the temporal range of *Thaumastosaurus* is limited to the Eocene (Vasilyan 2018). MAB19654 differs from Palaeobatrachidae (Roček et al. 2021) by relatively short metacarpals, the lack of ribs fused to vertebral diapophyses, rod-like sacral apophyses and the lack of a synsacrum. MAB19654 differs from Alytidae (Sanchíz y Gil de Avalle 1977; Bailon 1999; Roček 2013, therein Discoglossidae) by the absence of an alary process on the pterygoid, a straight humeral diaphysis, posterior diapophyses elongate, non-imbricated neural arches, absence of a free rib on V4, absence of transverse processes of the

urostyle, presence of rod-like sacral apophyses and the absence of a femoral crest. Lastly, MAB19654 differs from Bufonidae (Böhme 1977; Sanchíz y Gil de Avalle 1977; Bailon 1999; Ratnikov 2001) by a tooth-bearing maxilla, straight humeral diaphysis rod-like sacral apophyses, non-imbricated neural arches, a slender femur lacking a crest and a slender tibiofibula.

MAB19654 resembles Ranidae in the following characters (Böhme 1977; Sanchíz y Gil de Avalle 1977; Bailon 1999; Ratnikov 2001): tooth-bearing maxilla, dermal bones not sculpted, absence of an alary process of the pterygoid, non-imbricated neural arches, absence of free ribs, posterior apophyses elongate, cylindrical sacral apophyses, urostyle not fused to sacrum, absence of transverse processes of the urostyle, absence of a femoral crest, two tarsal bones that are free proximally and distally. Ranidae from early Oligocene of Europe have been referred to the genera *Pelophylax* (Sanchíz et al. 1993; Lemierre et al. 2022; Venczel et al. 2024) and *Rana* (Sanchíz et al. 1993).

Few osteological characters have been used to discriminate between modern water frogs *Pelophylax* and pond frogs *Rana* (G. Böhme 1977; M. Böhme 2001; Sanchíz et al. 1993; Bailon 1999; Ratnikov 2001; Blain et al. 2024). The humeral diaphysis in *Pelophylax* is more robust than in *Rana*, as the shaft in *Pelophylax* maintains roughly the same width as the humeral condyle and the shaft in *Rana* becomes narrower (Bailon 1999; Ratnikov 2001). Moreover, in male specimens, the crista medialis in *Pelophylax* remains low and does not reach midshaft unlike *Rana* (Bailon 1999; Ratnikov 2001). MAB19654 resembles the humeral morphology described for *Pelophylax*. Skulls of *Rana* are mediolaterally wider and anteroposteriorly shorter than in *Pelophylax* (Bailon 1999). The outline of the skull of MAB19654 more closely resembles that of *Pelophylax* kl. *esculentus* (figured in Ecker 1864) and *Pelophylax meriani* (Von Meyer 1860) than that of adult *Rana temporaria* (figured in Parker 1871). However, skull outline in fossil forms may be altered due to taphonomic processes (Sanchíz y Gil de Avalle 1977). Böhme (2001) utilised sacral angulation as a character, as their data implied that sacral angulation in *Pelophylax* is greater than in *Rana*. However, our data (Table 2; Supplementary File 2) did not find a significant difference between the two ranid genera. Lastly, *Rana* species have longer and more slender femora than *Pelophylax* (Bailon 1999). Given the relative shortness of the femur of MAB19654 even

with respect to other *Pelophylax* (Gubányi and Korsós 1992), reference to *Rana* seems inappropriate.

Fossil *Pelophylax* specimens have been attributed to *Pelophylax* kl. *esculentus*, *P. aquensis*, *P. meriani*, *P. pueyoi*, *P. quellebergi* and *P. barani* (e.g., Lemierre et al. 2022; Blain et al. 2023, 2024; Dufresnes et al. 2024). There were no osteological synapomorphies identified that allow a species-level determination. We thus refrain from assigning a species to MAB19654, and refer it to as *Pelophylax* sp. Moreover, major radiation events in European *Pelophylax* seem to have occurred from the Early Miocene onwards (Dufresnes et al. 2024). First, a clade containing *P. perezii* diverged from a clade with *P. ridibundus* and *P. lessonae* during the Early Miocene. A more exclusive clade with *P. lessonae* branched from the *P. ridibundus* clade during the Middle Miocene (Dufresnes et al. 2024). We deem reference of Oligocene *Pelophylax* specimens to *Pelophylax* kl. *esculentus* (e.g., Lemierre et al. 2022) to be invalid, as this klepton represents the fertile hybrid of *P. lessonae* and *P. ridibundus* (Berger 1973; Uzzell et al. 1976), and a klepton cannot precede the divergence of both of its parent species. A comprehensive review of Oligocene *Pelophylax* material is recommended before any specific diagnosis can be made.

Ecomorphological evolution in *Pelophylax*

Morphological evolution in European ranids has been generally slow and at a constant rate (Martínez-Gil et al. 2025). In particular, Bergmann's rule, i.e. the notion that body size increases with lower temperatures (Bergmann 1848) and the water conservation hypothesis, stating that ectotherms favourably attain larger size with lower precipitation rates (e.g., Gouveia and Correia 2016), best explain evolutionary trends within *Rana* species (Martínez-Gil et al. 2025). The same trends have been identified in *Pelophylax*, as body size is negatively correlated with primary production, temperature and precipitation – the genus attains maximum body size during glacial periods and smallest body size during interglacials and warm periods (Martínez-Monzón et al. 2022, 2023; Blain et al. 2024). Given the palaeogeographical overlap between *Rana* and *Pelophylax*, similar processes likely govern the macroevolutionary patterns of both genera throughout the Cenozoic.

Limb bone proportions are indicative of both mode of locomotion and microhabitat in frogs (Jorgenson and Reilly 2013; Enriquez-Urzelai et al. 2015; Lires et al. 2016; Citadini et al. 2018; Gómez and Lires 2019; Moen 2019; Buttner et al. 2020; Stepanova and Womack 2020; Petrović et al. 2021; Leavey et al. 2023; Pérez-Ben et al. 2024; Ponssa et al. 2025). In terms of limb bone metrics, MAB19654 most closely resembles *Pelophylax ridibundus* – as *P. perezii* and *P. lessonae* have significantly shorter calcaneus and longer femora, respectively (Table 2). Since no osteological metric of *P. ridibundus* divert significantly from the other extant taxa, and its femur to tibiofibular ratio also matches that of the fossil *P. pueyoi* (Sánchez y Gil de Avallé 1977), *P. meriani* (Von Meyer 1860), *P. aquensis* and MAB19654 (Table 2), the limb bone proportions of *P. ridibundus* are treated here as representative of early *Pelophylax*.

All three sampled extant *Pelophylax* species are highly aquatic (e.g., Wells 2007; Trochet et al. 2014; Freire Oliveira et al. 2017; AmphibiaWeb 2025). *P. perezii* has a relatively reduced calcaneus compared to the femur (Table 2). Elongation of the calcaneus is correlated with greater jumping ability (Leavey et al. 2023), suggesting poorer jumping performance in *P. perezii* compared to other *Pelophylax* species. There was not sufficient locomotion, dispersal or habitat data documented for *P. perezii* in the main amphibian trait databases (Trochet et al. 2014; Freire Oliveira et al. 2017) to substantiate this hypothesis. Generally, aquatic frogs like *Pelophylax* primarily use jumping to evade predators and not as their favoured mode of locomotion (e.g., Gans and Parsons 1966). *P. lessonae* has a distinctly longer femur in relation to the tibiofibula compared to the other extant *Pelophylax* species (Table 2), which likely reflects a derived character state (Fig. 10). Femur elongation occurs in aquatic frogs (Leavey et al. 2023). This is consistent with the observation that *P. lessonae* primarily displaces by swimming (Trochet et al. 2014). Moreover, the sacral angulation in *P. lessonae* is significantly lower than that of the other *Pelophylax* species, indicating poorer walking and hopping capabilities (Jorgenson and Reilly 2013; Leavey et al. 2023).

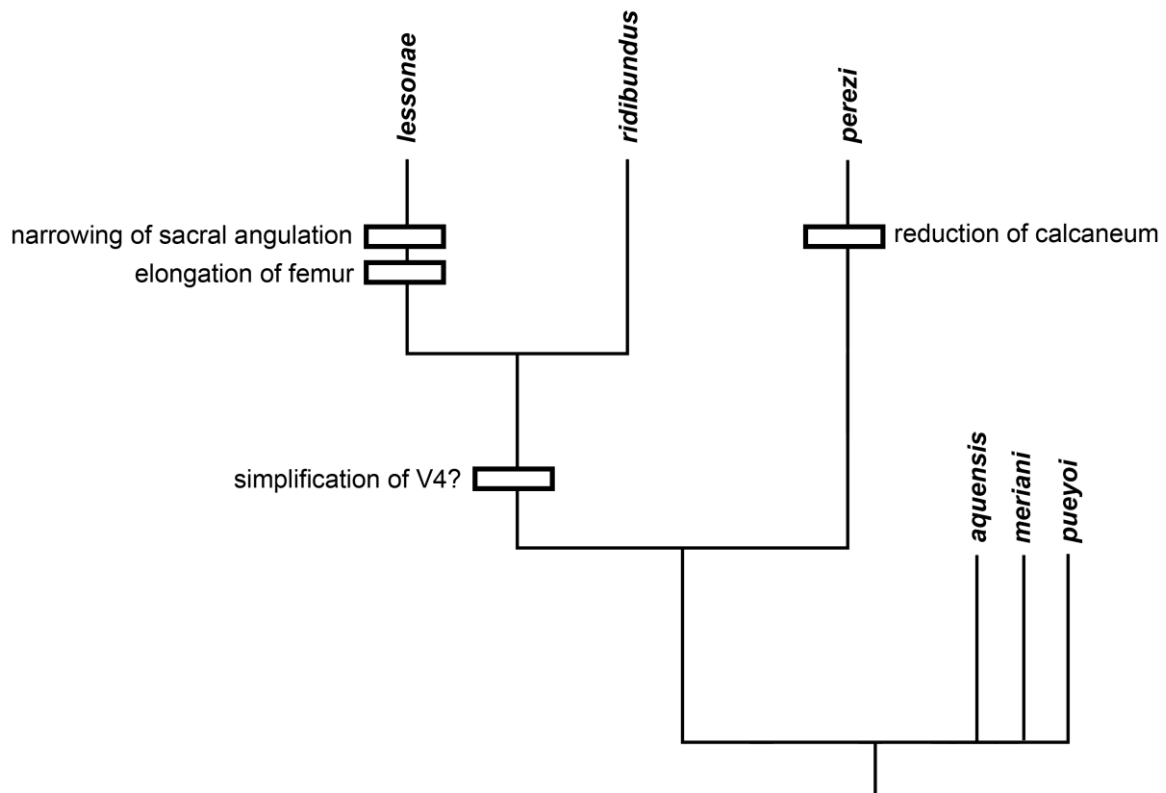


Figure 10. Hypothesised character acquisition on a simplified phylogenetic tree (adopted from Dufresnes et al. 2024). Since the phylogeny was based on molecular data and lacked fossil taxa, the fossil taxa here are placed in a basal polytomy.

Pelophylax species occupy a variety of habitats, from deciduous forests to semideserts and desert areas (AmphibiaWeb 2025). Large-scale studies on anuran microhabitat occupation do not discriminate between different types of aquatic habitats (e.g., Ponssa et al. 2025) and thus cannot be used to infer habitat preference in early *Pelophylax*. Extant *Pelophylax* species commonly co-occur sympatrically, but display specific habitat preferences; *P. ridibundus* prefers deeper waters with little vegetation, whereas *P. lessonae* favours shallow waters that dry out temporally (Pagano et al. 2001; Holenweg Peter et al. 2002; Wells 2007; Kolenda et al. 2024). Interestingly, *P. ridibundus* has an exceptionally high tolerance to salinity and can reproduce on the shores of the present-day Black Sea and Caspian Sea (Mollov 2020; AmphibiaWeb 2025). This indicates that *Pelophylax* species, and likely early *Pelophylax* such as MAB19654, could have been able to adapt to the brackish conditions of the early Oligocene Apt-Manosque-Fourcalquier basin (Gaudant 1978).

Using the largest osteological dataset of *Pelophylax* limb bone proportions to date, we show that the three sampled extant species display considerable ecomorphological variation and correlate this variation to mode of locomotion. This approach looks promising to explore morphological evolution within the widespread and speciose genus *Pelophylax* further, for example by including species from different geographical areas and microhabitats.

Methodologically, one should be careful regarding the type of preservation of the specimens used and not use different types of preservation interchangeably. We show that ratios measured from dry bone, cartilage-capped bone and living specimens can differ significantly (Table 2; Supplementary File 2). Moreover, taxonomically diverse studies typically limit the number of specimens per species. Given the intraspecific variance observed in frog limb ratios (Table 2), and the large number of osteological specimens that are present in museum collections, it is recommended to work with larger samples sizes.

Lastly, there is considerable variation observed in V4 morphology. MAB19654 displays a clear trapezoid morphology. Such a trapezoidal morphology of transverse processes of V4 has frequently been used as one of the osteological characters justifying taxonomical difference between extant *Pelophylax* and extinct species (Navás 1920, 1922; Sanchíz y Gil de Avalle 1977; Blain et al. 2023). All of the four defined morphologies (narrow parallel, wide parallel, spatulate and trapezoid) are observed in the three studied extant species (*P. lessonae*, *P. perezi*, and *P. ridibundus*). The more complex trapezoid and spatulate morphologies are far more common in *P. perezi* (75%). Simple parallel morphologies occur more frequently in the clade including *P. lessonae* (69.5%) and *P. ridibundus* (74%), with *P. lessonae* more frequently displaying narrow apophyses (52.5% narrow, 16.9% wide) and *P. ridibundus* more frequently displaying wider apophyses (58.6% wide, 15.5% narrow). Complex V4 might therefore be ancestral in *Pelophylax*, while the simplification of the V4 apophyses may be a derived trait for *P. lessonae* and *P. ridibundus*. Future studies should further explore the morphological evolution of V4, as this may prove to be a useful character for determining *Pelophylax* species in palaeontological and zooarchaeological contexts.

Conclusions

We describe a new male fossil ranid frog, MAB19654, from the early Oligocene of southern France and assign it to *Pelophylax* sp. Assignment to *Pelophylax* is based on the robust humerus bearing a low crista medialis that does not reach midshaft, skull shape and relatively short femur. However, there are insufficient osteological characters discriminating between fossil *Pelophylax* species. Nonetheless, MAB19654 represents one of the oldest known *Pelophylax* specimens and notably predates the major radiation events of the Miocene, shedding light on early *Pelophylax* osteology.

In terms of limb bone ratios, MAB19654 resembles the other sampled fossil *Pelophylax* species: *P. aquensis*, *P. pueyoi* and *P. meriani*. The femur to tibiofibula ratio in *Pelophylax lessonae* is significantly higher than in any other sampled *Pelophylax* species. In addition, the sacral angulation of *P. lessonae* is narrower than that of other *Pelophylax*. *Pelophylax perezi* has a significantly reduced tarsus relative to femur compared to other *Pelophylax* species. We did not find a significant difference in sacral angulation between the genera *Pelophylax* and *Rana*. The limb bone ratios of MAB19654 most closely resembles *Pelophylax ridibundus* among extant species. A shortening of the tarsus occurred in the lineage leading to *Pelophylax perezi*, while *Pelophylax lessonae* evolved a relatively more elongate femur and narrower the sacral apophyses.

Lastly, we show interspecific variation in the abundance of specific apophysial morphologies of V4 within *Pelophylax*. Simple parallel morphologies are common in the *Pelophylax ridibundus* + *Pelophylax lessonae* clade: *Pelophylax lessonae* often develops narrow V4 apophyses, while the apophyses in *Pelophylax ridibundus* are widened. On the other hand, complex spatulate and trapezoid morphologies appear more frequently in the early-branching *Pelophylax perezi*. Moreover, a trapezoid morphology is also present in MAB1954. Thus, complex V4 morphologies appear ancestral in *Pelophylax*, and looks to be a promising tool in distinguishing between *Pelophylax* groups.

Acknowledgements

We thank Wilma Wessels and Wout Krijgsman (Universiteit Utrecht, Utrecht, Netherlands) for their help with finding suitable palaeogeographic maps of the European Oligocene.

Florian Witzmann and Andreas Rassuly (Museum für Naturkunde, Berlin, Germany), Marta Calvo Revuelta (Museo Nacional de Ciencias Naturales, Madrid, Spain), and Damien Germain (Muséum national d'Histoire naturelle, Paris, France) are thanked for granting H-AB access to *Pelophylax* specimens under their custody. We are grateful to Auke Barnhoorn, Ellen Meijvogel-de Koning and their team from the Technische Universiteit Delft (Delft, Netherlands) for their help with the CT-scanning of specimen MAB19654. The research of H-AB is funded by projects PID2021-122533NB-I00 and PID2024-157622NB-I00 from the Spanish Ministry of Science and Innovation (MCIN/AEI/10.13039/501100011033/FEDER 'Una manera de hacer Europa'), by project GAČR 21-33751S of the Czech Science Foundation, and by the CERCA Program/Generalitat de Catalunya. H-AB belongs to the Consolidated Research Group 'Paleoecology of Pliocene and Pleistocene and Human Dispersals (Pal-Hum)', funded by projects 2021SGR-1238 (AGAUR-Generalitat de Catalunya) and 2023PFR-URV-01238 (URV). The IPHES-CERCA has received financial support through the "María de Maeztu" program for Units of Excellence (CEX2024-01485-M/funded by MICIU/AEI/10.13039/501100011033).

References

AmphibiaWeb. 2025. <<https://amphibiaweb.org>> University of California, Berkeley, CA, USA.

Accessed 22 Dec 2025.

Bailon S. 1999. Différenciation ostéologique des Anoures (Amphibia, Anura) de France. Fiches d'ostéologie animale pour l'archéologie Série C: Varia. Centre de Recherches Archéologiques du CNRS. ISSN: 0982-3840.

<https://hal.science/mnhn-03262226/>

Batsch AJ. 1796. Umriss der gesammten Naturgeschichte. Christian Ernst Gabler.

Berger L. 1973. Systematics and Hybridization in European Green Frogs of *Rana esculenta* Complex.

Journal of Herpetology 7: 1–10.

doi.org/10.2307/1562822

Bergmann C. 1848. Über die Verhältnisse der Wärmeökonomie der Thiere zu ihrer Grösse.

Vandenhoeck und Ruprecht.

Blain H-A and Arribas OJ. 2017. A description of the skeletal morphology of *Rana pyrenaica* (Anura: Ranidae), with comments on functional morphology, ecological adaptation and relationships with other Iberian ranids. Zootaxa 4319(3): 510–530.

doi.org/10.11646/zootaxa.4319.3.5

Blain H-A, Lózano-Fernández I and Böhme G. 2015. Variation in the ilium of central European water frogs *Pelophylax* (Amphibia, Ranidae) and its implications for species-level identification of fragmentary anuran fossils. Zoological Studies 54: 1–9.

doi.org/10.1186/s40555-014-0094-3

Blain H-A, Přikryl T, Cáceres I, Rodríguez-Salgado P, Martínez-Monzón A, Linares-Martín A, Lozano-Fernández I, Moreno-Ribas E, Grandi F, Oms O, Agustí J, Campeny Vall-Llosera G and Gómez de Soler B. 2024. Skeletal taphonomy of the water frogs (Amphibia: Anura) from the Pit 7/8 of the Pliocene Camp dels Ninots site (Caldes de Malavella, NE Spain). Historical Biology 36(9): 1951–1978.

doi.org/10.1080/08912963.2023.2237998

Blain H-A, Přikryl T, Moreno-Ribas E and Canudo JI. 2023. The first discovery of in situ *Pelophylax pueyoi* (Amphibia: Anura) from the late Miocene of Libros Konservat-Lagerstätte (Teruel, Spain). *Journal of Vertebrate Paleontology* 42(2): e2162410.
doi.org/10.1080/02724634.2022.2162410

Böhme G. 1977. Zur Bestimmung quartärer Anuren Europas an Hand von Skelettelementen. *Wissenschaftliche Zeitschrift der Humboldt-Universität zu Berlin, Mathematisch-Naturwissenschaftliche Reihe* 26: 283–300.
<https://pascal-francis.inist.fr/vibad/index.php?action=getRecordDetail&idt=PASCALGEODEBRGM7820371413>

Böhme M. 2001. The oldest representative of a brown frog (Ranidae) from the Early Miocene of Germany. *Acta Palaeontologica Polonica* 46: 119–224.
<https://agro.icm.edu.pl/agro/element/bwmeta1.element.agro-article-25bc125a-dba8-4d00-9d4a-39ce272fd2da>

Buttimer SM, Stepanova N and Womack MC. 2020. Evolution of the unique anuran pelvic and hindlimb skeleton in relation to microhabitat, locomotor mode, and jump performance. *Integrative and Comparative Biology* 60(5): 1330–1345.
doi.org/10.1093/icb/icaa043

Chan KO and Brown RF. 2017. Did true frogs ‘dispersify’? *Biology Letters* 13: 20170299.
doi.org/10.1098/rsbl.2017.0299

Citadini JM, Brandt R, Williams CR and Gomes FR. 2018. Evolution of morphology and locomotor performance in anurans: relationships with microhabitat diversification. *Journal of Evolutionary Biology* 31: 371–381.
doi.org/10.1111/jeb.13228

Coquand H. 1845. Sur la découverte faite dans les plâtrières d’Aix d’une grenouille fossile. *Bulletin de La Société Géologique de France* 2: 393–394.

Costa E, Garcés M, Sáez A, Cabrera L and López-Blanco M. 2011. The age of the “Grande Coupure” mammal turnover: New constraints from the Eocene–Oligocene record of the Eastern Ebro Basin (NE Spain). *Palaeogeography, Palaeoclimatology, Palaeoecology* 301: 97–107.

doi.org/10.1016/j.palaeo.2011.01.005

Coster P and Legal S. 2021. An Early Oligocene Fossil Lagerstätten from the Lacustrine Deposits of the Luberon UNESCO Global Geopark. *Geoconservation Research* 4(2): 604–612.

doi.org/10.30486/GCR.2021.1915524.1068

Crochet P-A, Dubois A, Ohler A and Tunner H. 1995. *Rana (Pelophylax) ridibunda* Pallas, 1771, *Rana (Pelophylax) perezi* Seoane, 1885 and their associated klepton (Amphibia, Anura): morphological diagnoses and description of a new taxon. *Bulletin du Muséum national d'histoire naturelle* 4(17): 11–30.

doi.org/10.5962/p.290311

Destombes JP. 1962. Description géologique du bassin oligocène de Manosque-Forcalquier (Luberon oriental). *Bulletin du service de la carte géologique de la France* 68(266): 461–568.

<https://insu.hal.science/insu-00904953/>

Ducieux J-L, Hugueney M and Truc G. 1985. La Formation des Calcaires et Lignites de Sigonce (Oligocène moyen, Bassin de Forcalquier, Alpes-de-Haute-Provence): datation à l'aide des mammifères; reconstitution des milieux de dépôts. *Geobios* 18: 109–114.

[doi.org/10.1016/s0016-6995\(85\)80183-2](https://doi.org/10.1016/s0016-6995(85)80183-2)

Duméril C. 1805. *Zoologie analytique, ou Méthode naturelle de classification des animaux, rendue plus facile à l'aide de tableaux synoptiques*. Allais, Paris, 386 pp.

doi.org/10.5962/bhl.title.11646

Dufresnes C and Mazepa G. 2020. Hybridogenesis in Water Frogs. *eLS* 1: 718–226.

doi.org/10.1002/9780470015902.a0029090

Dufresnes C, Monod-Broca B, Bellati A, Canestrelli D, Ambu J, Wielstra B, Dubey S, Crochet P-A, Denoël M and Jablonski D. 2024. Piecing the barcoding puzzle of Palearctic water frogs (*Pelophylax*) sheds light on amphibian biogeography and global invasions. *Global Change Biology* 30: e17180.

doi.org/10.1111/gcb.17180

Ecker A. 1889. *The anatomy of the frog*. Translated by G. Haslam. Oxford at the Clarendon Press. 449 pp.

doi.org/10.5962/bhl.title.7851

Enriquez-Urzelai U, Montori A, Llorente GA and Kaliontzopoulou A. 2015. Locomotor Mode and the Evolution of the Hindlimb in Western Mediterranean Anurans. *Evolutionary Biology* 42(2): 199–209.

doi.org/10.1007/s11692-015-9311-1

Fitzinger LJ. 1843. *Systema reptilium: fasciculus primus: Amblyglossae*. Braumüller & Seidel.

doi.org/10.5962/bhl.title.4694

Freire Oliveira B, São-Pedro VA, Santos-Barrera G, Penone C and Costa GC. 2017. Data Descriptor: AmphibiO, a global database for amphibian ecological traits. *Scientific Data* 4: 170123.

doi.org/10.1038/sdata.2017.123

Frost D. 2025. Amphibian Species of the World 6.2, an Online Reference. Accessed 23-11-2025.

doi.org/10.5531/db.vz.0001

Gans C and Parsons TS. 1966. On the Origin of the Jumping Mechanism in Frogs. *Evolution* 20: 92–99.

doi.org/10.2307/2406151

Gaudant J. 1978. Sur une nouvelle espèce de Poissons Téléostéens Cyprinodontiformes de l'Oligocène des environs de Manosque (Alpes-de-Haute-Provence). *Géologie Méditerranéenne* 5(2): 281–290.

doi.org/10.3406/geolm.1978.1050

Gaudant J, Nel A, Nury D, Véran M and Carnevale G. 2018. The uppermost Oligocene of Aix-en-Provence (Bouches-du-Rhône, Southern France): A Cenozoic brackish subtropical Konservat-Lagerstätte, with fishes, insects and plants. *Comptes Rendus Palevol* 17: 460–478.

doi.org/10.1016/j.crpv.2017.08.002

Georgalis GL, Prendini E and Roček Z. 2023. New information on the Eocene frog *Thaumastosaurus* (Anura, Pyxicephalidae) from the Phosphorites du Quercy, France. *Zoological Journal of the Linnean Society* 199: 744–770.

doi.org/10.1093/zoolinnean/zlad047

Gómez RO and Lires AI. 2019. High ecomorphological diversity among Early Cretaceous frogs from a large subtropical wetland of Iberia. *Comptes Rendus Palevol* 18: 711–723.

doi.org/10.1016/j.crpv.2019.07.005

Gouveia SF and Correia I. 2016. Geographical clines of body size in terrestrial amphibians: water conservation hypothesis revisited. *Journal of Biogeography* 43(10): 2075–2084.

doi.org/10.1111/jbi.12842

Gubányi A and Korsós Z. 1992. Morphological analysis of two Hungarian water frog (*Rana lessonae-esculenta*) populations. *Amphibia-Reptilia* 13: 235–243.

doi.org/10.1163/156853892x00445

Haeckel E. 1866. *Generelle Morphologie der Organismen. Zweiter Band. Allgemeine Entwicklungsgeschichte der Organismen.* Berlin, Georg Kramer.

Holenweg Peter A-K, Reyer H-U and Abt Tietje G. 2002. Species and sex ratio differences in mixed populations of hybridogenetic water frogs: The influence of pond features. *Écoscience* 9: 1–11.

doi.org/10.1080/11956860.2002.11682684

Holsbeek G and Jooris R. 2010. Potential impact of genome exclusion by alien species in the hybridogenetic water frogs (*Pelophylax esculentus* complex). *Biological Invasions* 12: 1–13.

doi.org/10.1007/s10530-009-9427-2

Ivany LC, Patterson WP and Lohmann KC. 2000. Cooler winters as a possible cause of mass extinctions at the Eocene/Oligocene boundary. *Nature* 407: 887–890.

doi.org/10.1038/35038044

Jorgenson ME and Reilly SM. 2013. Phylogenetic patterns of skeletal morphometrics and pelvic traits in relation to locomotor mode in frogs. *Journal of Evolutionary Biology* 26(5): 929–943.

doi.org/10.1111/jeb.12128

Kolenda K, Kaczmarski M, Żurawska J and Ogielska M. 2024. Decline of *Pelophylax lessonae* in mixed populations of water frogs over the last 50 years. *The European Zoological Journal* 91: 94–104.

doi.org/10.1080/24750263.2023.2300284

Kruzhkova YI and Kovalenko EE. 2010. Regularities of Morphogenesis of the Coccygeosacral Articulation in Anura. *Russian Journal of Developmental Biology* 41(2): 111–121.
doi.org/10.1134/s1062360410020074

Laloy F, Rage J-C, Evans SE, Boistel R, Lenoir N and Laurin M. 2013. A Re-Interpretation of the Eocene Anuran *Thaumastosaurus* Based on MicroCT Examination of a ‘Mummified’ Specimen. *PLoS ONE* 8(9): e74874.
doi.org/10.1371/annotation/f7988d67-24b9-493c-9aef-c5c715948a1e

Leavey A, Ruta M, Richards CT and Porro LB. 2023. Locomotor, ecological and phylogenetic drivers of skeletal proportions in frogs. *Journal of Anatomy* 243: 404–420.
doi.org/10.1111/joa.13886

Lemierre A, Folie A, Bailon S, Robin N and Laurin M. 2021. From toad to frog, a CT-based reconsideration of *Bufo servatus*, an Eocene anuran mummy from Quercy (France). *Journal of Vertebrate Paleontology* 41(3): e1989694.
doi.org/10.31233/osf.io/p6kse

Lemierre A, Gendry D, Poirier M-M, Gillet V and Vullo R. 2022. The oldest articulated ranid from Europe: A *Pelophylax* specimen from the earliest Oligocene of Chartres-de -Bretagne (NW France). *Journal of Vertebrate Paleontology* 42(4): e2191663.
doi.org/10.1080/02724634.2023.2191663

Lemierre A and Orliac MJ. 2025. Lissamphibians from Dams (Quercy, SW France): Taxonomic identification and evolution across the Eocene-Oligocene transition. *Palaeovertebrata* 48: e3.
[doi: 10.18563/pv.48.1.e3](https://doi.org/10.18563/pv.48.1.e3)

Licht A, Coster P, Botté P, Kaya M, Deschamps P, Guihou A and Legal S. 2024. Sedimentology and chronostratigraphy of the Apt Basin, Southeastern France: lacustrine response to late Paleogene cooling and regional rifting. *BSGF - Earth Sciences Bulletin* 195(1): 22.
doi.org/10.1051/bsgf/2024019

Lires AI, Soto IM and Gómez RO. 2016. Walk before you jump: new insights on early frog locomotion from the oldest known salientian. *Paleobiology* 42(4): 612–623.
doi.org/10.1017/pab.2016.11

Martínez-Gil H, Kaliontzopoulou A and Enriquez-Urzelai U. 2025. Different Macroevolutionary Trajectories Lead to Contrasting Ecogeographical Patterns in Two Widespread Frog Radiations. 2025. *Global Ecology and Biogeography* 34:e70109.
doi.org/10.1111/geb.70109

Martínez-Monzón A, Pšikryl T, Sánchez-Bandera C, Bisbal-Chinesta JF, Agustí J, Campeny Vall-Llosera G, Gómez de Soler B and Blain H-A. 2023. Inferring eco-climate parameters for the Pliocene Climate Optimum using frog body size as a new proxy. *Lethaia* 56(2): 1–12.
doi.org/10.18261/let.56.2.8

Martínez-Monzón A, Sánchez-Bandera C, Fagoaga A, Oms O, Agustí J, Barsky D, Solano-García, Jiménez-Arenas JM and Blain H-A. 2022. Amphibian body size and species richness as a proxy for primary productivity and climate: The Orce wetlands (Early Pleistocene, Guadix-Baza Basin, SE Spain). *Palaeogeography, Palaeoclimatology, Palaeoecology* 586: 110752.
doi.org/10.1016/j.palaeo.2021.110752

Mayer M, Hawlitschek O, Zahn A and Glaw F. 2013. Composition of twenty Green Frog populations (*Pelophylax*) across Bavaria, Germany. *Salamandra* 49: 31–44.
[https://www.semanticscholar.org/paper/Composition-of-twenty-Green-Frog-populations-\(-\)-%2C-Mayer-Hawlitschek/815033d4da3c9219574ce3f98a633c0716e465aa](https://www.semanticscholar.org/paper/Composition-of-twenty-Green-Frog-populations-(-)-%2C-Mayer-Hawlitschek/815033d4da3c9219574ce3f98a633c0716e465aa)

Moen DS. 2019. What Determines the Distinct Morphology of Species with a Particular Ecology? The Roles of Many-to-One Mapping and Trade-Offs in the Evolution of Frog Ecomorphology and Performance. *The American Naturalist* 194(4): 81–95.
doi.org/10.1086/704736

Mollov IA. 2020. Frogs at the Sea – Unusual Breeding Site of *Pelophylax ridibundus* (Pallas, 1771) (Amphibia: Anura) at the Black Sea Coast (Bulgaria). *Ecologia Balkanica* 12(2): 203–205.
https://openurl.ebsco.com/EPDB%3Agcd%3A13%3A12940781/detailv2?sid=ebsco%3Aplink%3Ascholar&id=ebsco%3Agcd%3A148089556&crl=c&link_origin=scholar.google.nl

Navás L. 1920. Fósiles del Oligoceno de Libros (Teruel). *Ibérica*. Año. VI (326):282–283.

Navás L. 1922. Algunos fósiles de Libros (Teruel). Boletín de la Sociedad Ibérica de Ciencias Naturales. 21:52–61.

Orr PJ, Adler LB, Beardmore SR, Furrer H, McNamara ME, Peñalver-Mollá E and Redelstorff R. 2016. “Stick ‘n’ peel”: Explaining unusual patterns of disarticulation and loss of completeness in fossil vertebrates. *Palaeogeography, Palaeoclimatology, Palaeoecology* 457: 380–388.
doi.org/10.1016/j.palaeo.2016.05.024

Oustalet E. 1874. Recherches sur les insectes fossiles des terrains tertiaires de la France. G. Masson.

Pagano A, Joly P, Plénet S, Lehman A and Grolet O. 2001. Breeding habitat partitioning in the *Rana esculenta* complex: The intermediate niche hypothesis supported. *Écoscience* 8(3): 294–300.
doi.org/10.1080/11956860.2001.11682656

Palcu DV and Krijgsman W. 2023. The dire straits of Paratethys: Gateways to the anoxic giant of Eurasia. Geological Society, London, Special Publications.
doi.org/10.1144/sp523-2021-73

Parker WK. 1871. On the structure and development of the skull of the common frog (*Rana temporaria*, L.). *Proceedings of the Royal Society of London* 19: 137–211.
doi.org/10.5962/bhl.title.95807

Petrović TG, Vukov T and Kolarov NT. 2021. Patterns of correlations and locomotor specialization in anuran limbs: association with phylogeny and ecology. *Zoology* 144: 125864.
doi.org/10.1016/j.zool.2020.125864

Pérez-Ben C, Lires AI and Gómez RO. 2024. Frog limbs in deep time: is jumping locomotion at the roots of the anuran Bauplan? *Paleobiology* 50: 96–107.
doi.org/10.1017/pab.2023.23

Piveteau J. 1927. Etudes sur quelques amphibiens et reptiles fossiles. *Annales de Paléontologie*, 16, 1–47.

Ponssa ML, Terán CL, Folly H, Fratani J and Abdala V. 2025. Ecomorphology of Anurans: The Challenge of Ecological Categories and Locomotor Modes. *Journal of Experimental Zoology Part B: Molecular and Developmental Evolution*.

doi.org/10.1002/jez.b.23330

Rafinesque CS. 1814. Fine del prodromo d'erpetologia siciliana. *Specchio Delle Scienze, o, Giornale Enciclopedico Di Sicilia*, 2, 102–104.

Rage J-C. 1984. Are the Ranidae (Anura, Amphibia) known prior to the Oligocene? *Amphibia-Reptilia* 5: 281–288.

doi.org/10.1163/156853884x-005-03-09

Rage J-C and Bailon S. 2005. Amphibians and squamate reptiles from the late early Miocene (MN 4) of Béon 1 (Montréal-du-Gers, southwestern France). *Geodiversitas* 27(3): 413–441.

<https://hal.science/hal-00019636v1>

Rage J-C and Roček Z. 2003. Evolution of anuran assemblages in the Tertiary and Quaternary of Europe, in the context of palaeoclimate and palaeogeography. *Amphibia-Reptilia* 24: 133–167.

doi.org/10.1163/156853803322390408

Ratnikov VY. 2001. Osteology of Russian toads and frogs for paleontological researches. *Acta Zoologica Cracoviensa* 44: 1–23.

<https://agro.icm.edu.pl/agro/element/bwmeta1.element.agro-article-8edab78d-8584-4317-a1e2-1a5b4594df12>

Reig O. 1958. Propositiones para una nueva macrosistemática de los anuros (nota preliminar). *Physis* 21(60): 109–118.

Roček Z. 2013. Mesozoic and Tertiary Anura of Laurasia. *Palaeobiodiversity and Palaeoenvironments* 93: 397–439.

doi.org/10.1007/s12549-013-0131-y

Roček Z, Rage J-C and Venczel M. 2021. Fossil frogs of the genus *Palaeobatrachus* (Amphibia: Anura). *Abhandlungen der Senckenberg Gesellschaft für Naturforschung* 575: 1–151.

<https://hal.science/hal-03990379/>

Roček Z and Wuttke M. 2010. Amphibia of Enspel (Late Oligocene, Germany). *Palaeobiodiversity and Palaeoenvironments* 90:321–340.

doi.org/10.1007/s12549-010-0042-0

Roček Z, Wuttke M, Gardner JD and Bhullar B-AS. 2014. The Euro-American genus *Eopelobates*, and a re-definition of the family Pelobatidae (Amphibia, Anura). *Palaeobiodiversity and Palaeoenvironments* 94: 529–567.

doi.org/10.1007/s12549-014-0169-5

Sanchíz B. 1998. *Encyclopedia of Paleoherpétology, part 4, Salientia*. Verlag Dr. Friedrich Pfeil, München.

Sanchíz B, Schleich HH and Esteban M. 1993. Water Frogs (Ranidae) from the Oligocene of Germany. *Journal of Herpetology* 27(4): 486–489.

doi.org/10.2307/1564847

Sanchíz y Gil de Avalle F. 1977. *Nuevos anfibios del Neogeno y Cuaternario de Europa. Origen, desarrollo y relaciones de la batrachofauna Española*. [Unpublished doctoral dissertation] Universidad Complutense de Madrid.

<https://hdl.handle.net/20.500.14352/39982>

Saporta G de. 1891. *Recherches sur la végétation du niveau Aquinien de Manosque*. Librairie polytechnique.

<https://gallica.bnf.fr/ark:/12148/bpt6k98631p/>

Sauvage HE. 1880. Notice sur les poissons tertiaires de Céreste (Basses-Alpes). *Bulletin de la Société géologique de France* 8(3): 439–451.

Schuler M and Sittler C. 1976. Données paléoclimatiques à l'aube des temps néogènes en Haute Provence (France). *Géologie Méditerranéenne* 3(3): 155–159.

doi.org/10.3406/geolm.1976.971

Stepanova N and Womack MC. 2020. Anuran limbs reflect microhabitat and distal, later-developing bones are more evolutionarily labile. *Evolution* 74(9): 2005–2019.

doi.org/10.1111/evo.13981

Trochet A, Moulherat S, Calvez O, Stevens VM, Clobert J and Schmeller DS. 2014. A database of life-history traits of European amphibians. *Biodiversity Data Journal* 2: e4123.

doi.org/10.3897/bdj.2.e4123

Uzzell T, Günther R and Berger L. 1976. *Rana ridibunda* and *Rana esculenta*: A Leaky Hybridogenetic System (Amphibia Salientia). *Proceedings of the Academy of Natural Sciences of Philadelphia* 128: 147–171.

<https://www.jstor.org/stable/4064723>

Vasilyan D. 2018. Eocene Western European endemic genus *Thaumastosaurus*: new insights into the question “Are the Ranidae known prior to the Oligocene?”. *PeerJ* 6:e5511.

doi.org/10.7717/peerj.5511

Venczel M, Codrea V and Fărcaș C. 2013. A new palaeobatrachid frog from the early Oligocene of Suceag, Romania. *Journal of Systematic Paleontology* 11(2): 179–189.

doi.org/10.1080/14772019.2012.671790

Venczel M, Codrea VA, Solomon A, Fărcaș C and Bordeianu M. 2023. Lissamphibians from the late Eocene – early Oligocene transition of the Transylvanian Basin (Romania). *Historical Biology* 37(7): 1679–1691.

doi.org/10.1080/08912963.2024.2392719

Vianey-Liaud M, Comte B, Marandat B, Peigne B, Rage J-C and Sudre J. 2014. A new early late Oligocene (MP 26) continental vertebrate fauna from Saint-Privat-des-Vieux (Alès Basin, Gard, Southern France). *Geodiversitas* 36(4): 565–622.

doi.org/10.5252/g2014n4a4

Von Meyer H. 1860. *Palaeontographica. Beiträge zur Naturgeschichte der Vorwelt. Siebenter Band.* Verlag von Theodor Fischer, Cassel

doi.org/10.1515/9783112666142-017

Wells KD. 2007. *The ecology and behavior of amphibians.* The University of Chicago Press, Chicago and London. 1400 pp.

doi.org/10.7208/chicago/9780226893334.001.0001

Yuan Z-Y, Zhou W-W, Chen X, Poyarkov NA, Chen H-M, Jang-Liaw N-H, Chou W-H, Matzke NJ, Iizuka K, Min M-S, Kuzmin SL, Zhang Y-P, Cannatella DC, Hillis DM and Che J. 2016. Spatiotemporal Diversification of the True Frogs (Genus *Rana*): A Historical Framework for a Widely Studied Group of Model Organisms. *Systematic Biology* 65(5): 824–842.

doi.org/10.1093/sysbio/syw055